

# Outlook on Plasmalemmal Vesicles (Caveolae)

*Klaus Fiedler*

E-mail: [contact@klausfiedler.ch](mailto:contact@klausfiedler.ch)

Words (Text): 6800

## Abstract

Caveolae are involved in several physiological roles of importance to human health. Genome-wide association studies have indicated a caveolin-1/2 (Cav1/Cav2) relation to heart rate and atrial fibrillation, an electrophysiological process. When applying effect sizes and frequencies in variants of the Cav1/Cav2 genomic region, the UK Biobank evaluates atrial fibrillation as the most important, hitherto discovered population measure of their variation. A model of caveolae is presented in this outlook that takes into account the previous work on protein modelling, electron cryomicroscopy and protein isolation of caveolae, primarily from an animal source, and suggests, that the wealth of tissue-culture data is not always consistent with claims on the characterization of caveolae from plasmalemmal-vesicle-enriched lung endothelia. Caveolae are covered by an abundant associated coat-like structure containing prevalent Cav1 and reggie-1/flotillin-2 (Flot2) that range from 8:1 – 15:1 in protein stoichiometry. Flot2 may have a vault-shaped structure that covers the flask-shaped invagination since a highly significant structural similarity of reggie-1/flotillin-2 to the major vault protein (MVP) is elucidated.

## A geometric model of a caveola

Ever since the discovery of caveolin (Glenney & Soppet 1992) the structure of caveolins has not been solved. Structural proposals have been made (Fig. 1 A). The here suggested model of a caveola is drawn to scale (magnification approx. 420'000): The edges could be covered by ESA/reggie/flotillin (yellow) (flotillin was quantified relative to caveolin in stoichiometry) and drawn with average diameter at expected or shorter length and caveolin is covering a part of each face. The caveolin density would amount to a concentration of 10 mmole/l in the plane of the membrane bilayer considering its 4 nm size in the membrane normal direction. At this concentration, an average cell would contain approximately 30 million caveolae if equivalent at this level. In extension, it seems likely that caveolin is 5'000-fold more concentrated in the membrane bilayer than the average 63 nm<sup>3</sup> cellular protein in the cytoplasm and since the protein is not very abundant, the number of caveolae per cell is correspondingly smaller. A thermodynamic solution would predict that at this concentration, a  $\Delta G^\circ$  (Gibbs free energy) of low -1.3 kcal/mole in the binding reaction could generate an equilibrium distribution of 50% monomers and dimers each of encaged caveolins. This suggests that membrane reactions are strongly driven towards association of integral- or also membrane-associated proteins and afford particular attention to the low-affinity solution biochemistry of protein detergent extracts. Moreover, it has been estimated in a geometric model that at the size of 10  $\mu$ m distance of diffusion to encounter another molecule, assuming the circular dimerization interface of 1 nm in radius, caveolin would benefit from combined diffusion at the membrane interface and within the cytoplasm to meet,

should soluble molecules exist (Adam & Delbrück 1968) (**Fig. 1 B**). Likely this is only to occur, if the diffusion constants within the membrane and cytoplasm vary by only a factor of 950 (see old data) which had not been explored in detail. Of course, in biogenesis caveolin has been shown to be translated at the ER (endoplasmic reticulum) and subsequently is to multimerize on its way to the cell surface; secretion of the protein has also been found. It is of note, that the reaction interface for dimerization and higher order oligomerization of caveolin is small compared to soluble factors since the protein is restricted in its degrees of rotational freedom within the membrane. It is likely that one or another surface accessible structural feature of caveolins takes part in oligomerization that does not require large tertiary structural stabilization. This notion is maintained due to the solubility of caveolin-1 (Cav1) which is known to be resistant to various detergents, forms soluble oligomers early in the secretory pathway as shown by Kurzchalia and colleagues, and is resistant to SDS (sodium dodecyl sulfate) and likely urea in oligomerization in SDS-polyacrylamide gel electrophoresis (SDS-PAGE) assaying or is easily found to renature from urea in the presence of SDS (unpublished observation). The view of Lisanti and co-workers on the oligomer-oligomer interactions that would be referring to later, multiple oligomer formation and/or multimerization and involving the C-terminal residues, could equally apply to initial oligomerization as shown; related to this mechanism, the predicted membrane domain would be involved in hetero-oligomerization as shown in Cav1 and caveolin-2 (Cav2) (Das et al. 1999). In this model, caveolin is graphed as two nonamers (green) with approximately 2 nm protrusion from the membrane bilayer (light blue) (**Fig. 1 A**). Contacts between nonamers are occurring at the perimeter of the disk-shaped structure, homophilic interactions of secondary structural elements in nonamer formation are likely to form in the central disk area, and are stabilized by long chain fatty acylation (Monier et al. 1996). The caveolin-scaffolding domain in the molecular model would not fold into an  $\alpha$ -helical structure as presumed (Fernandez et al. 2002) but rather be extended in structure proximal to the  $\alpha$ -helical domain that includes part of the CRAC (cholesterol recognition amino-acid consensus) motif, likely consistent with this observation (Hoop et al. 2012). See Seminar (Fiedler 2018) for a drawing how the scaffolding stretch would be closely apposed to the more distal membrane span in the proposed structural model.

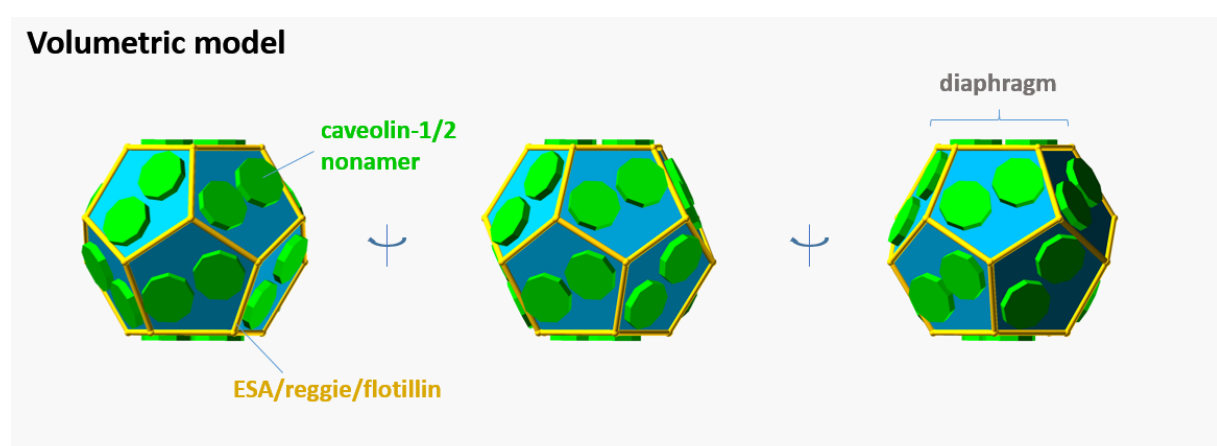
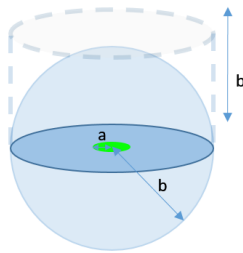


**Fig. 1 A Model of a Caveola**

## Models of diffusion predict roles of membrane-anchored supercomplexes



It is here assumed that molecules are distributed uniformly between two concentric spheres with radii  $a$  and  $b$ . In three dimensions the outer surface of the sphere (green) adsorbs molecules on first contact, the outer sphere reflects molecules (light blue). The new diffusion constant is measured in the two-dimensional model when molecules encounter the equatorial plane (dark blue). The target area (green) would represent complexed caveolin molecules tethered to other caveolins or interacting molecules that would be stably positioned.

### Ratio of diffusion times

$$\frac{\tau^{(3,2)}}{\tau^{(3)}} = \left\{ \frac{1}{3} \cdot \frac{D^{(2)}}{D^{(3)}} \left[ Y_1 \left( \frac{b}{a} \right) \right]^2 \frac{b}{a} \left( 1 - \frac{a}{b} \right)^2 \right\}^{-1}$$

The mean combined time of diffusion  $\tau^{(3,2)}$  is illustrated by introducing the cylinder of height

$$Y_1 \text{ is dependent on } \frac{b}{a} \text{ and is derived from Bessel functions } J_0 \left( \frac{a}{b} y \right) Y_1(y) - Y_0 \left( \frac{a}{b} y \right) J_1(y) = 0$$

Thus the diffusion time depends on  $\frac{b}{a}$  and  $\frac{D^{(2)}}{D^{(3)}}$

*Superscripts refer to the dimension in space*

**Fig. 1 B Geometric Model of Diffusion**

## Caveolin structure is inferred from EM and protein analysis

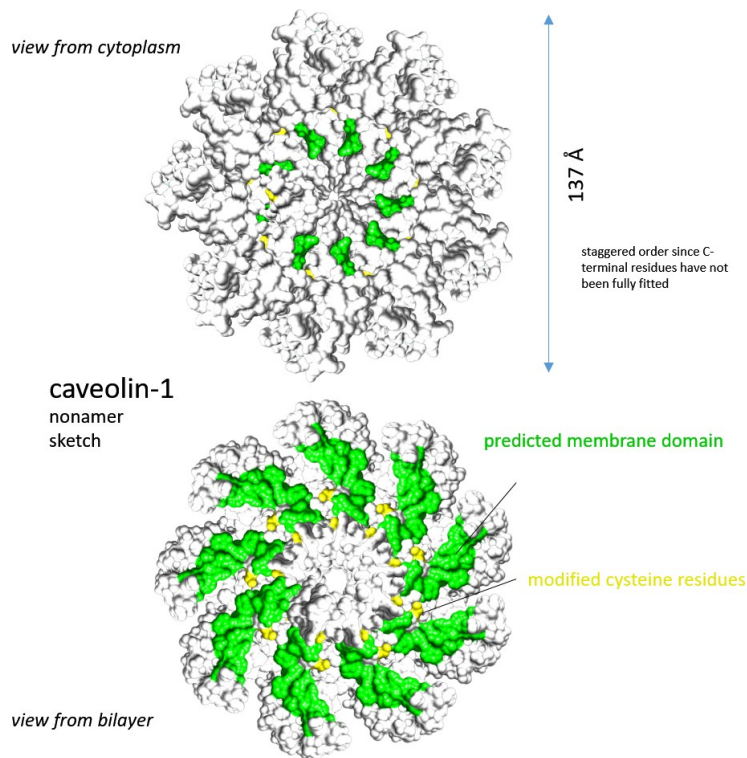


**Fig. 1 C Structural Model of Caveolin-1**

## Model of reggie-1 - the Major Vault Protein (MVP) p100 and SPFH-domain were compared

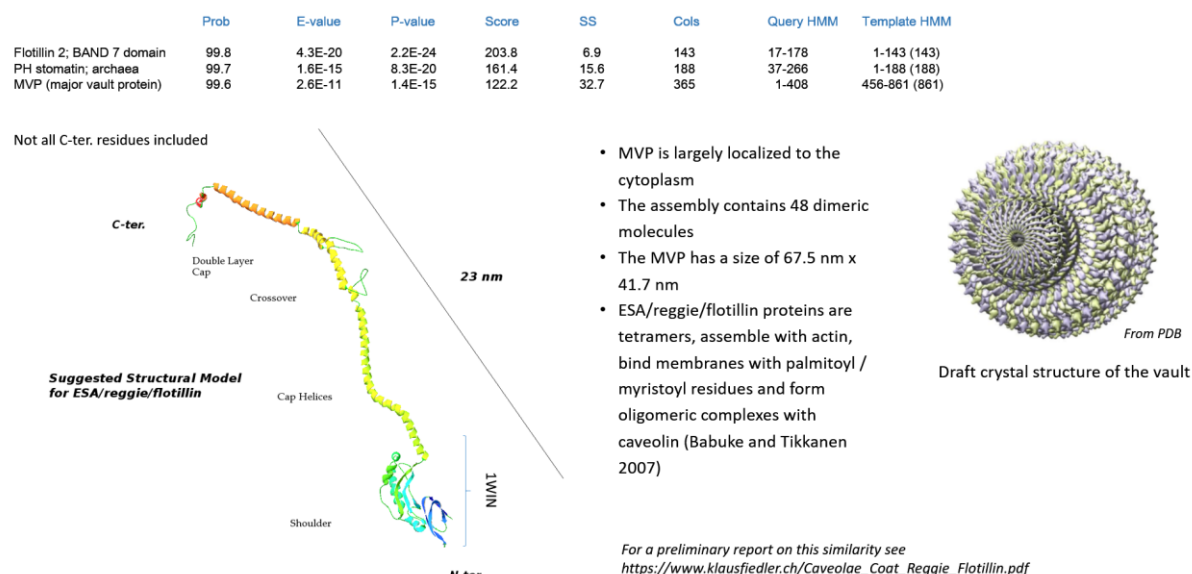


**Fig. 1 D Model of Reggie-1/Flotillin-2**

**Figure 1: A geometric model of a caveola.** (A) Dodecahedral examples of a caveola cage. Previously, caveolae have been described with a “spiral-shaped” coat of unknown function and composition. Protein evidence, obtained by purification of plasmalemmal vesicles “caveolae” with immunoisolation supports and specific anti-caveolin-1 $\alpha$  antibodies, indicates that a major part of caveolae is constituted by two proteins, caveolin-1 $\alpha$  and ESA/reggie-1/flotillin-2. The protein model is drawn to scale using volumetric data of cav1 and flot2 protein models. The dodecahedral vesicular morphology has been suggested by structural analysis of Stoeber et al. (Stoeber et al. 2016). The overall composition was, however, not analyzed in this study. Three different views are shown, two of which are rotated by 20° and 40° each. Reggie/flotillin is colored in yellow, the caveolin disk in green. (B) A geometric model of diffusion suggests, that soluble caveolin molecules that may occur in the cytoplasm, would collide and complex with pre-existing membrane-bound molecules more often, if colliding first with the membrane and then forming complexes of caveolin-1 oligomers, or the like. (C) The structural model of caveolin-1 is shown in a sketch with similar dimensions to the nonamer analyzed in Whiteley et al. (Whiteley et al. 2012). The dodecahedral structure is plotted in dimensions that match the size of caveolin and alternative stoichiometry is utilized to visualize single nonamer caveolin-disks per face of the dodecahedron. Although protein density of caveolin-1 has been determined by high-resolution light microscopy, the density of ESA/reggie-1/flotillin-2 has not been analyzed. Caveolin density in cellular membranes (Khater et al. 2018) would pin-point towards the model shown in (A) harboring two caveolin-1/caveolin-2 disks per vesicle dodecahedral face. Caveolin-1 would form approximately 76% of the nonamer with presumably 24% of other caveolins (caveolin-2) and 16 nonamers would cover 8 faces of the dodecahedron, whereas 4 faces would form the diaphragmal area. Alternatively, if only one face of the dodecahedron would constitute or generate the diaphragmal or diaphragm-free attachment with the plasma membrane, only 56% of each nonamer would consist of caveolin-1 whereas the rest would be constituted by other proteins in the here suggested face-nonamer stoichiometry. (D) The reggie-1/flotillin-2 protein from rat (also named ESA) was modelled (see (Fiser & Sali 2003)) and found to match an elongated shaped protein, the Major-Vault Protein (MVP) (Anderson et al. 2007). MVP is found to oligomerize to a 48 dimeric-protein containing particle of unknown function, the major vault particle that is found in the cytoplasm. It may bear similarity in shape and possibly assembly properties to ESA/reggie-1/flotillin-2. For direct comparison to the result previously obtained (Fiedler 2008b), the scores for human reggie-1 are indicated in the panel and presented as Supplementary Fig.1.

None of these working hypotheses have been confirmed by detailed structural data, yet, a caveolin-3 (Cav3) nonamer has been described by Kitmitto and colleagues (Whiteley et al. 2012) (see Fig. 1 C). In 2008 it was found that caveolin-1 has a distinct structural similarity (by a Hidden Markov Model

comparison HHpred) to PITP $\alpha$  (phosphatidyl-inositol transfer protein  $\alpha$ ) which would suggest lipid-binding functions of Cav1, and would leave room for speculation about its enzymatic role and substrate channeling of fatty acyls/lipids/cholesterol (Fiedler 2008a). Furthermore, similarly shaped particles of Cav1 and the cavin-1 (PTRF) were also characterized (Stoeber et al. 2016) and have inspired the drawing of the dodecahedron above, however, the high-resolution architecture and molecular composition is yet not fully understood. Modeling of Cav1-associated proteins or their homologues is leading to interesting results (Fig. 1 D). The putative homology of reggie-1/flotillin-2 to the major vault protein (MVP) summarized in (Fiedler 2008b) suggests in this way that caveolae could be covered by a shell of reggie/flotillin filaments that sterically mold the flask-shaped caveolae.

### Immunoisolation data

The sparsity of reggie/flotillin relative to Cav1 in my immunoisolation, would suggest that not the full surface is covered as shown (Figs. 1 A, 2 C, 2 F) since the model volume would account for only approximately one fourteenth of the entire vesicle coat. The shell of the vesicle is predicted to be filled by  $\alpha$ -helical reggie/flotillin molecules with an approximate diameter of 1.6 nm and is graphed in the appropriate relative size and stoichiometry to Cav1 or Cav1 bound to Cav2. Unless the immunoisolation was inefficient in retaining the molecule on the vesicle and it was set free, only a “porous” cage of reggie/flotillin proteins would sculpt and bind to the caveolar surface; this has been envisioned to present a homologous reaction to the molding of the barrel structure formed by the major vault protein (Fig. 1 D) but may not occur without the co-factors that have lately been described, the cavin proteins that have been identified in myc-transformed cells (Hill et al. 2012). These proteins could, however, not be characterized in our high-resolution immunoisolation from rat lung endothelia (Chatenay-Rivauday et al. 2004) and it remains speculative as to the abundance of cavin proteins in caveolae in different organs. Despite a demonstrated role of cavin proteins in shaping the caveolae (Hill et al. 2008) a function in lipid metabolism or signaling may be suggested in lipidomics (see [lipidgenie.com](http://lipidgenie.com)).

Lisanti and co-workers had previously shown the interaction of Cav1 and reggies/flotillins, others had denied the existence of hetero-oligomers of these factors since they had conducted interaction analyses (binding to a post-nuclear supernatant) using green fluorescent protein (GFP)-reggie/flotillin (Ludwig et al. 2010) and isolated low amounts of Cav1. For unbiased observers, it was thus impossible to judge the required geometry of interactions for membrane- or membrane-associated-proteins since reggie/flotillin was tagged with GFP in the latter experiment and Cav1 would, moreover, interact within the membrane bilayer or in its vicinity. Appreciable quantities of both, Cav1 and actin were found to interact with GFP-reggie/flotillin following a first detergent wash with Triton, and it was yet not practicable to differentiate the different modalities in this series of experimental treatments (raft isolation or low-affinity interaction).

This leaves the possibility that true interactions of low-affinity that occur within or close to the plane of the plasma membrane have been found, that may, since Cav1 was abundant in isolated vesicles and included very little Cav2 similar to apical trans-Golgi network-derived vesicles from kidney epithelial cells of dog (MDCK) (Scheiffele et al. 1998), form a coat of Cav1 and reggies/flotillins in apical endothelial caveolae from rat lung (see also caveolae in Cav1 and Cav2-/- mice (Drab et al. 2001; Razani & Lisanti 2001; Razani et al. 2002a, Razani et al. 2002b)). The abundance of Cav1 had not been generalized to other Golgi-derived carrier vesicles. In our experiments using plasma membrane isolated by the established silica method, we had found that 6 and 8% of reggie-1/flotillin-2 and reggie-



2/flotillin-1, respectively, would specifically bind to caveolin-1 $\alpha$  in immunoprecipitates which is, considering that reggie/flotillins localize also to non-caveolar microdomains, a substantial quantity (Chatenay-Rivauday et al. 2004).

### Expression level of RNAs

The protein and RNA expression has today been followed-up at present high single-cellular resolution. Results from an analysis of more than 100'000 cells from 20 different mouse organs suggest the very abundant expression of Cav1 and Cav2 in endothelial cells. The cells here were scrutinized by single-cell RNA sequencing (mean expression data) (Schaum et al. 2018) and are summarized in the Supplement (Supplementary Table 1). Clustering in 10 groups by five genes suffices to sub-group most endothelia into two heterogeneous groups, cardiac muscle cells, B and T cells; skeletal muscle cells were not included. The heart smooth muscle cells may include "cardiac muscle" which according to historical knowledge are similar to cardiac type at the root of the pulmonary artery and vein and are shown to express some Cav3 and, as expected, Cav1 and 2. This is just noted since expression data harbor many unknowns but surprisingly a wealth of knowledge interpreted in an elaborate way.

Consistent with these findings it has been found that endothelial lineages (venous and capillary endothelial cells) are expressing Cav1 and Cav2 and can be modeled in a pseudotime trajectory, these lineages included lymphatic endothelial, arterial endothelial and endocardial cells (Cao et al. 2019). In the latter study Tbx5, a T-box transcription factor known to be involved in heart development (see (Moskowitz et al. 2007)), was found to delineate development of the endocard as well and it may be, that Cav1/Cav2 expression is intricately involved in regulating mechanosignaling and adhesion processes since this is, furthermore, found in cardiomyocytes. Both cell types, endocardial cells and myocytes, may be involved in conduction cell biogenesis found at later stages, and these circumstances had explained the atrial conduction defects associated with Cav1/Cav2 (Ellinor et al. 2012; Holm et al. 2010; Vatta et al. 2006) without providing further mechanistic knowledge.

### Model of desaturases and $M_w$ of partially unknown associated- and desaturase proteins

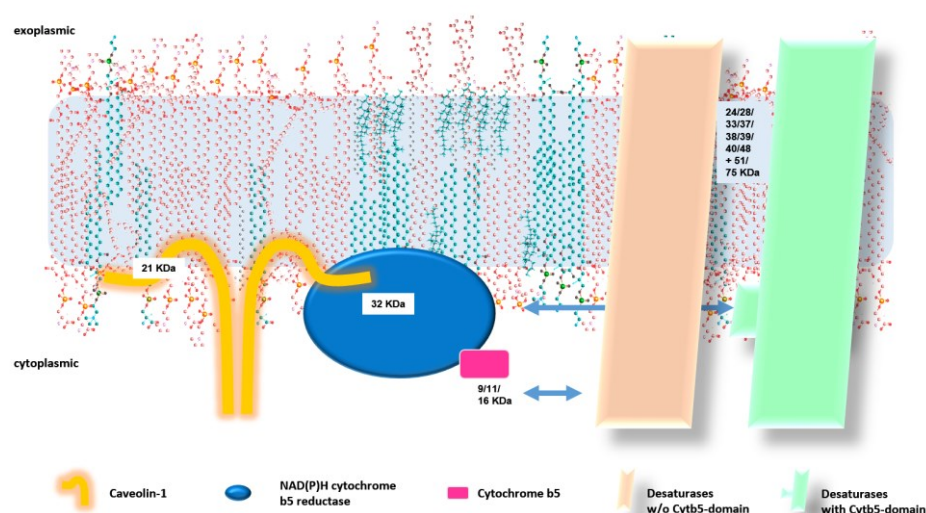


**Fig. 2 A Desaturation of Acyl-Chains**

## Lipid desaturases: FADS1/2 reactions

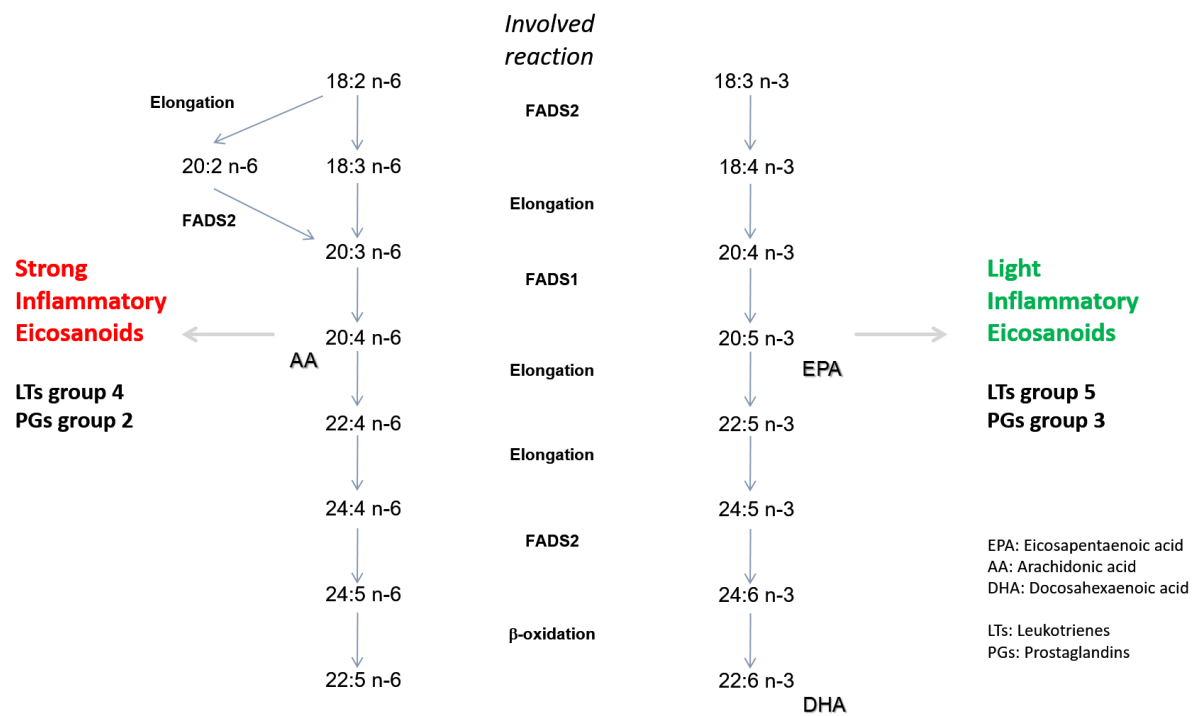


Fig. 2 B Omega Fatty Acid Biosynthesis

## Caveolae: Pleiotropic effects arise in lipid metabolism and signaling

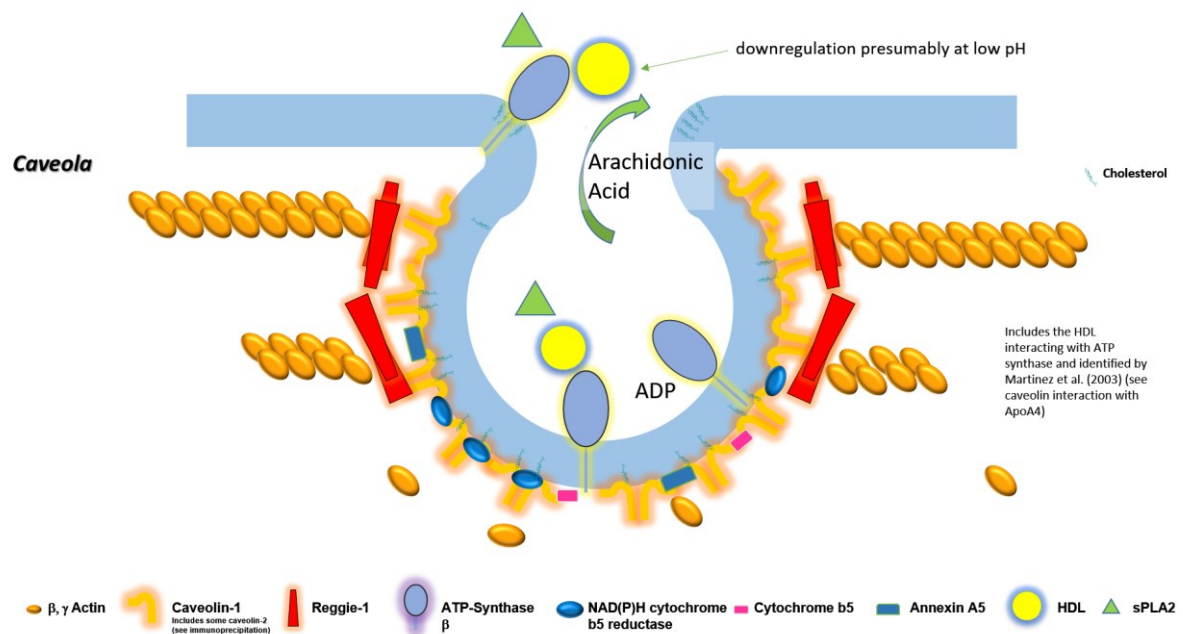


Fig. 2 C Extended Roles of Caveolae in Signaling

# Prostaglandin biosynthesis: Catalytic turnover

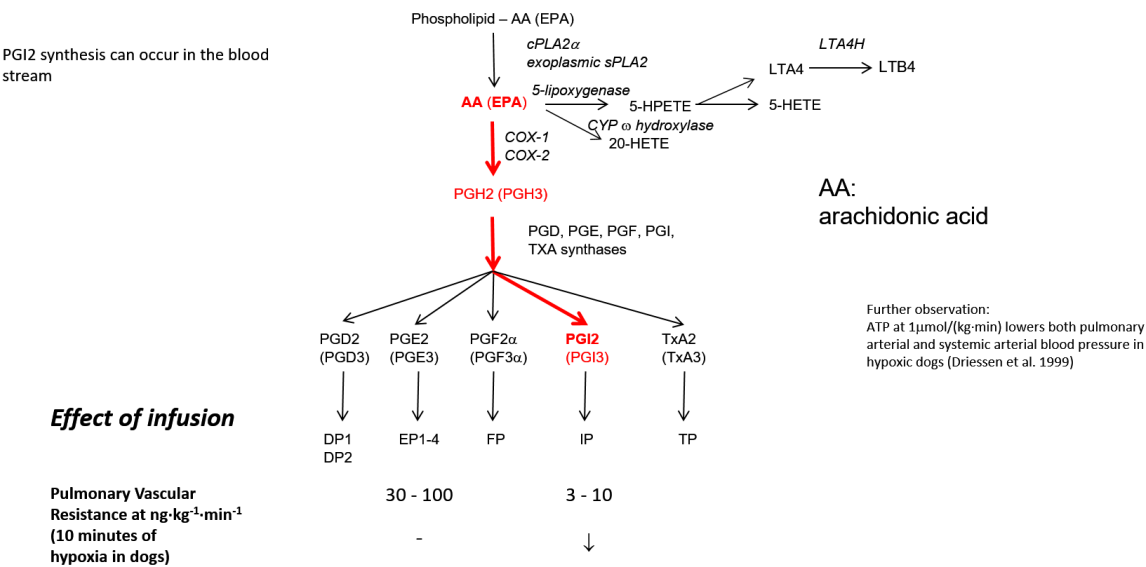


Fig. 2 D Prostaglandin Biosynthesis After AA Infusion

# Overlap of loci of caveolins and apolipoprotein A 4 with standard lipid traits

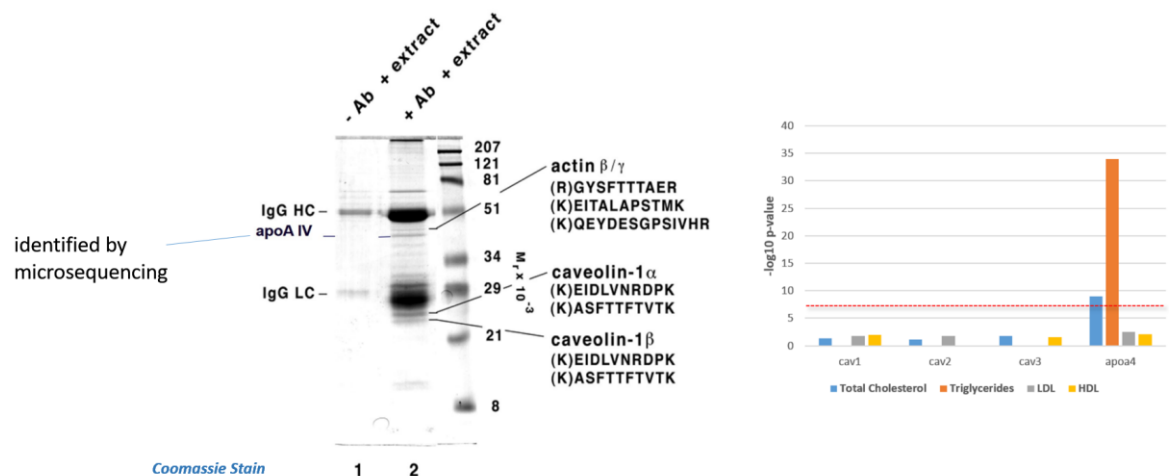
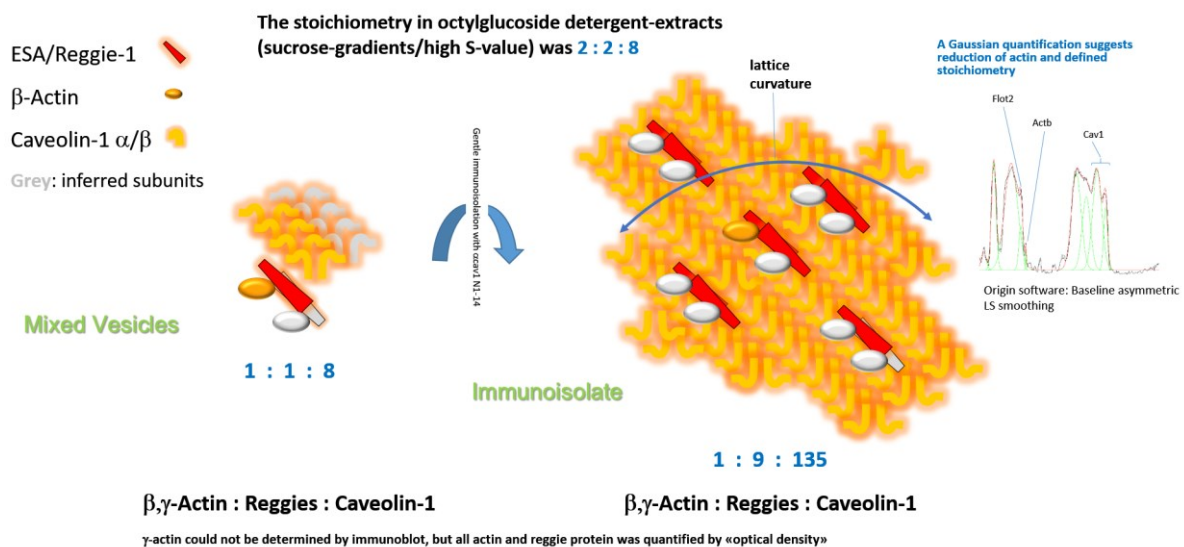


Fig. 2 E Caveolin-1 Interaction with ApoA 4



## Stoichiometry of the caveolae molecular coat



**Fig. 2 F Caveolae and Possible Relation to Reggies**

**Figure 2: Desaturation and a role of caveolae.** Desaturation reactions involve enzymes interacting with cytochromes or not requiring the interacting co-factors (A). For illustration, the omega-3/-6 fatty-acid (B) and link to eicosanoid (prostaglandins, leukotrienes, thromboxanes) biosynthetic pathways are shown. To demonstrate the role of caveolae in lipid signaling some known factors (not all from identical cell types) are summarized in (C); the multitude of findings on caveolae signaling through the cell cytoplasm are not described in this Outlook. It should be of note, that not all subunits of ectopic ATP-synthase have been determined. The biosynthesis of prostaglandins, leukotrienes and thromboxane from intermediates (arachidonic acid (AA) etc.) is shown in (D). A twist to Cav1 function has been discovered with its role in cholesterol efflux from cells that had been described by Fielding et al. and could relate to the novel caveolin interaction with ApoA 4 (apolipoprotein A4) (E). A genome-wide association study (GWAS) result is shown for the comparison of caveolins with ApoA 4 (Willer et al. 2013). (G) Results obtained by immunoisolation were quantified with the Origin software statistics and a gaussian mixture model to show the abundance and stoichiometry in caveolin-1 (Cav1), ESA/reggie-1/flotillin-2 (Flot2) and β-actin (Actb).

## Caveolae are proposed to be involved in fatty-acid desaturation

Lipid and fatty-acid desaturation is involved in, for example, omega-3 and -6 fatty-acid biosynthesis, some of these are produced in low amounts in humans and are taken up from a nutritive source (Fig. 2 A). In this reaction precursors are converted to Δ5, Δ6-, Δ9-CoA-acyls and other chains by elongation and to cholesterol and plasmalogens. Therein, phospholipids are also purportedly converted to more saturated acyl-chain containing lipids. A soluble fatty acid desaturase (FADS3) had been described that is localized to cyto- and exoplasmic structures (Blanchard et al. 2014) in addition to the more classical FADS1/2. With respect to the more ancient reggie/flotillin proteins that are even predicted to form large macromolecular complexes in bacteria, Riento et al. have analyzed sphingolipids in Flot1/- and Flot1/2/- knockout mice (Riento et al. 2018) and found the interesting interaction of sphingosine-1-phosphate levels in various tissues. The bacterial association of reggie/flotillin orthologues (or homologues) in specialized domains had been shown in this recent work (García-Fernández et al.

2017). This could relate to lipid signaling or metabolism and would be similar to caveolae and raft functions in eukaryotes. Lipid bodies are furthermore suggested to be involved in this reaction in higher organisms (Ostermeyer et al. 2004). **Fig. 2 B** illustrates the omega-3/-6 fatty-acid and link to eicosanoid (prostaglandins, leukotrienes, thromboxanes) biosynthetic pathways. Surprisingly, coupling-factor 6 (CF6; gene name Atp5pf) of ectopic plasma-membrane ATP synthase is involved in regulation of prostacyclin biosynthesis (Osanai et al. 2001) and caveolin-2 has been found to co-localize with secreted phospholipase A<sub>2</sub> (sPLA<sub>2</sub>) in several cell types (Murakami et al. 1999) linking the enzymatic roles of ectopic ATP synthase to vasoregulation. The former study showed that intravenous injection of recombinant CF6 protein in rats increased blood pressure dose-dependently within seconds and lasted for minutes. Although this demonstration of blood pressure regulation by ectopic ATP synthase was a convincing argument for the involvement of the prostacyclin signaling reaction, the kinetics of its desensitization remained unexplored. It is known from some in vitro assays that include pharmacologically triggered vasoregulation, and adenosine-receptors of the P2X class. This scenario may for example, also point towards the short half-life of the lipidic signaling mediator in the work of Osanai et al. of approximately 2 min and the intricate regulation of cytoplasmic reactions. Further, this may allude to rapid pH changes and adjustments in the proposed ATP hydrolysis reaction (surmised technically for the results (Martinez et al. 2003)) which occurs locally by surface diffusion by hops of protons from interacting groups to interacting groups as well as rather slow, by diffusion from one side of a cell to the opposite membrane within the time of a few minutes.

When it comes to the role of HDL (see **Fig. 2 E**), it would be of interest to further elucidate the intricate relation to phospholipases that are sometimes anchored to the cellular bilayer, bound to lipoprotein particles or found as soluble proteins. A study of Bousserouel et al. recently established a link of cytosolic and secreted phospholipase activities by applying arachidonyl trifluoromethyl ketone (AACOCF<sub>3</sub>), since in the presence of IL1 $\beta$  and AACOCF<sub>3</sub>, sPLA<sub>2</sub> activity in smooth muscle cells was strongly diminished (Bousserouel et al. 2003). Further functional cross-talk of these phospholipases had been shown by Balsinde et al. in macrophages (Balsinde et al. 1998). For a review on sPLA<sub>2</sub>s, the insight of which could be combined with these findings of Osanai et al., including the metabolic and inflammatory isoform in particular, see (Murakami et al. 2015).

To demonstrate the role of caveolae in lipid signaling some known factors (not all from identical cell types) are summarized in (**Fig. 2 C**). The biosynthesis of prostaglandins, leukotrienes and thromboxane from intermediates (arachidonic acid (AA) etc.) is shown in (**Fig. 2 D**). A twist to Cav1 function has been discovered with its role in cholesterol efflux from cells that had been described by the Fieldings (Fielding & Fielding 2000) and could relate to the novel caveolin interaction with ApoA 4 (apolipoprotein A4) that we had described in exceptional technical conditions and shown in several seminars (**Fig. 2 E**); this experiment has been carried through in a series of experiments similar to the published work (Chatenay-Rivauday et al. 2004) back in 1999 and was utilizing the buffer conditions of 40 mM octyl- $\beta$ -D-glucoside, EDTA, PBS, PMSF and protease inhibitors. The physiological role of these findings has not been fully elucidated, the ApoA 4 protein we had found is specialized since the large part of it is found as soluble protein in blood serum, wherein a monomer-dimer equilibrium exists (Deng et al. 2012); it is of note that Cav1, 2 and 3 had previously not been found to associate with standard lipid traits, the results of Willer et al. in a genome-wide association study (GWAS) are shown for the comparison with ApoA 4 (Willer et al. 2013). The flotillin/reggie protein Flot1 that was abundant on sucrose-gradients from detergent extracts of P1 lung membranes, obtained by lung perfusion, is the flotillin/reggie protein that has shown significant differences in lipid traits in this GWAS in humans

- Flot2, the abundant protein in caveolae, has not demonstrated this relationship. For our analysis presented here and mentioned above (**Fig. 1 A**), results obtained by immunoisolation were quantified with the Origin software statistics and a gaussian mixture model to show the abundance and stoichiometry in caveolin-1, ESA/reggie-1/flotillin-2 and  $\beta$ -actin (**Fig. 2 F**). The stoichiometry could be described with a ratio of 1 to 9 to 135 for  $\beta$ -actin to reggies/flotillins to caveolin-1.

### Liver apolipoproteins correlate with plasma lipid amounts

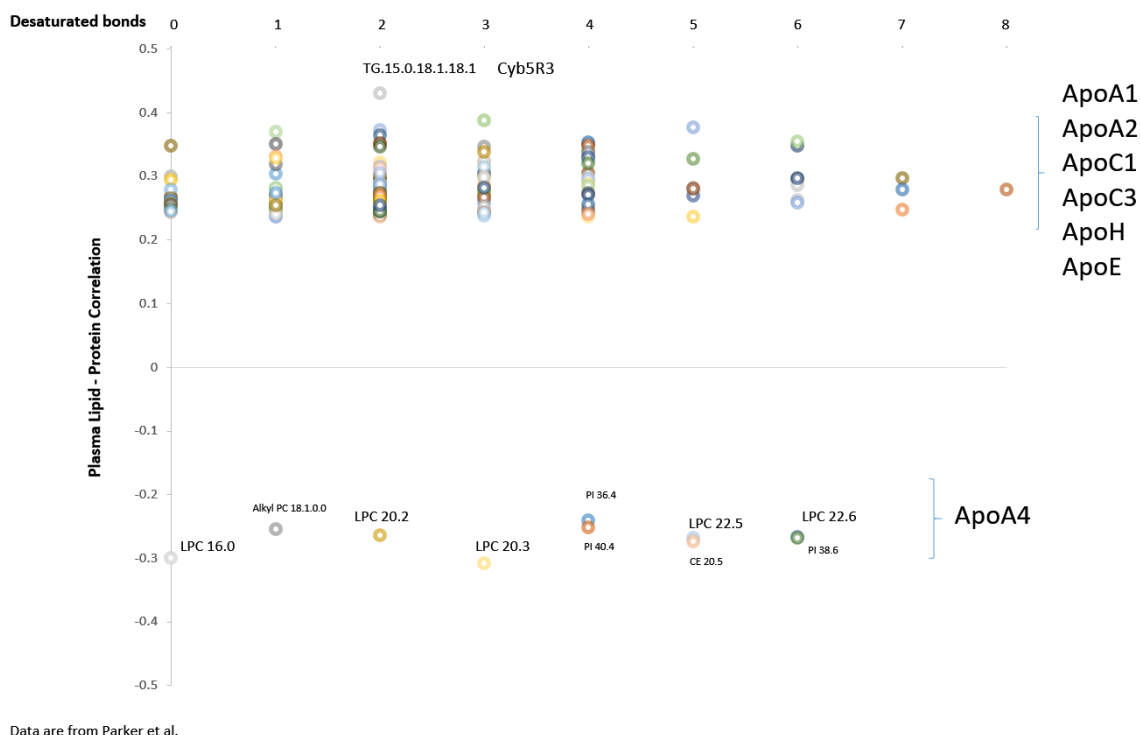


**Figure 3: Caveolae and indications for a function in specialized lipid metabolism and regulation.** A recent study in lipidomics demonstrated a connection of liver protein quantities of the apolipoprotein ApoA4 and plasma lysolipids that inversely correlated (Parker et al. 2019). The graph shows the number of desaturated bonds in the x-direction and biweight midcorrelations in the y-direction. Separate data points are indicated with various coloring, Cyb5R3 is added for comparison and is found to positively correlate with the quantities of triacylglycerides (highest correlating shown). Lipids in this analysis included triacylglyceride (TG), free cholesterol (COH), cholesterol ester (CE), diacylglycerol (DG), sphingomyelin (SM), ceramide (Cer), phosphatidylcholine (PC), phosphatidylethanolamine (PE), phosphatidylinositol (PI), alkyl-phosphatidylcholine (PC (O)) and lysophosphatidylcholine (LPC).

### ATP synthase, its biosynthetic pathway and a role in vasosignaling?

Surprisingly, coupling-factor 6 of mitochondrial ATP synthase which is localized to the plasma membrane has pointed towards a role of caveolae (see our Golgi and caveolae proteomics and abstracts of 1999) in blood pressure regulation since injection of the factor into blood rapidly affected the pressure (Osanai et al. 2001). Also here, lipids were implicated since the prostacyclin signaling reaction was altered. Consistent with above assumptions, studies in Cav1  $-/-$  mice have shown, that both, the amount of desaturated phospholipids in embryonic fibroblasts and the amount of eicosanoid release (prostaglandin E2 and LTB4) upon stimulation of macrophages in serum-free medium was

reduced (Astudillo et al. 2011; Le Lay et al. 2009) which suggests that indeed Cav1 is involved in their turnover and/or biosynthetic pathway. The relationship of prostacyclins to lipid desaturation is seen in biochemical pathways and provided by correlative evidence. It may be of note, that the recent analysis of plasma lipids and their comparison to liver proteomics has alluded to the interesting role of apolipoprotein A4 (ApoA4) in plasma amounts of lysolipids (Parker et al. 2019) (Fig. 3). In this elaborate study this finding has not been explained. Would it be a chance finding that desaturated lysolipids in plasma inversely correlated with liver amounts of ApoA4 and not with quantities of other apolipoproteins? The vote is still out and would cast a light on the true function of the ApoA4 that had been little studied. Strikingly in this study, NADH-cytochrome b5 reductase (Cyb5R3) amounts correlated positively (biweight midcorrelation) with the quantity of triacylglycerides (TGs) in plasma and consistently demonstrated this behavior the more desaturated the TGs were ( $r$  (Bicor.,Desat.) = 0.383 [0.124-0.624],  $p=0.028$ , the highest correlating TG (Bicor.) is shown;  $q<0.05$  for all indicated proteins and lipids (others not shown). Although the function of Cyb5R3 in lipid metabolism was thought to be established, more recent work has pointed towards its role in nitric-oxide signaling (see below) (Straub et al. 2012). Yet, the role of the previously identified Cav1-associated HDL (high-density lipoprotein), found to be secreted from pancreatic acinar cells (Liu et al. 1999) had not been clarified, and may be intricately related to a role of both, Cav1 and Cyb5R3, in lipid metabolism and/or signaling.

Let's return to the basic proteome to determine and discuss caveolae functions: Just as annexin 6, today established to be involved in mechanotransduction in sensory neurons in mouse, the annexin 5 that we described to be abundant in rat caveolae (see Fig. 2 C and 5 B), may be involved in mechanosignaling in the blood vascular endothelia (Raouf et al. 2018). The role of caveolae in trafficking had not been convincingly demonstrated: Whereas uptake of SV40 virus involved caveolar vesicles (visualized by GFP-tagging of Cav1) (Pelkmans et al. 2001), it was also found, that the uptake implicates turnover of the GFP-tagged caveolin protein and degradation in the endosomal pathway (Hayer et al. 2010). For caveolae in endothelia, Cav1 was required in hydrostatic pressure-mediated junctional protection in mouse myocardial endothelial cells, and the protein kinase C activator PMA (phorbol myristate) showed dependence on Cav1 for upregulation of permeability (dextran flow) (Müller-Marschhausen et al. 2008; Waschke et al. 2006). In microvascular beds in mice, the permeability found in brain, is proposed to involve authentic caveolae as transcellular carriers. Yet, in the latter experiments a characterization of the identity of all types of plasmalemmal vesicles had not been carried through and conclusions of the study were based on a double-mutant background. It could not be excluded that an interplay of Cav1 and Mfsda2 (major facilitator super family domain containing 2a), a lysolipid transporter studied in these Cav1<sup>-/-</sup>, Mfsda2<sup>-/-</sup> mice, may affect the regulation of protein kinase C (Andreone et al. 2017; Sando & Chertihin 1996). Overall, the interesting study suggested an intricate role of lysolipids in caveolae function but it may be too early to pinpoint towards the exact interplay, and functions of cholesterol and GM1 in caveolae dynamics had not been clarified until recently (Hubert et al. 2020) and would now strikingly indicate the caveolar role of the lipid-cell surface buffer and not of a transport vehicle.

The actin cytoskeleton had been described in the substance exchange across the endothelial cell layer and was found to be involved (Waschke et al. 2004). Furthermore, hypotheses describing caveolae function have been based on lipid raft isolation and analysis of protein content in numerous other studies. Yet, the lipid raft isolation technique that was used, usually allowed to assign factors to a subcellular localization by selecting for a property of density and/or detergent-insolubility only and could thus not suit the unequivocal localization to caveolae. With respect to the signaling role of

caveolae, it is well established that trimeric G(q) protein subunits are equally enriched in caveolae immunoisolates than ESA/reggie-1/flotillin-2 prepared from rat lung plasmalemma similarly to our procedure (Fiedler 2012; Oh & Schnitzer 2001). This is found, when converting the enrichment quantification to numbers comparable to the way of the analysis of ESA/reggie-1/flotillin-2 enrichment in caveolae.

The "non-conventional" insertion of ATP synthase at the ER, or scission of mitochondrial vesicles (coupled to further membrane fission and/or fusion and diffusion events and possibly topology inversion) followed by membrane transport and secretion, may be a proof of a signaling pathway at the plasma membrane that had not been discussed in previous work. ATP synthase could serve the extracellular ATP biosynthesis in caveolae with functions in paracrine and/or autocrine signaling (Chatenay-Rivauday et al. 2004; Fiedler 2002). ATP synthase at the cell surface, also named an ectoenzyme, was surprisingly shown to indeed produce ATP from ADP despite the possible absence of the complete mitochondrial eukaryotic respiratory chain as the driving force. The components of the respiratory chain may, however, provide a source of additional factors since it was itself recently shown to be functional within exosomes which are extracellular vesicles (Bruschi et al. 2016). Moreover, others have described ATP synthase as an apolipoproteinA 1 binding protein or to be involved in mechanosignaling in line with the proposed function as an "autacoid synthase" (Martinez et al. 2003; Yamamoto et al. 2007).

### **Genetic evidence for a role of caveolin-1/2 in cardiac disease**

Genetics and system-wide interactome analysis of caveolin-1/2 has allowed to conclude that caveolae must be involved in mechanisms that pertain to physiological dysregulation in atrial fibrillation and blood pressure (see references within) (Ellinor et al. 2012) (Figs. 4 C-E). The population attributable score (Fig. 4 A) can interestingly be generated from UK Biobank data, and confirms recent genetic evidence that Cav1 is involved in forming a risk (benefit at higher expression levels) for atrial fibrillation and flutter from GWAS results (rs55883210 and linked rs10271007, Table 1). This score is similar to relative risk versus attributable risk which is a parameter used in epidemiology, and may be utilized to describe the importance of GWAS data in a population-wide sense. Top 10 scores are shown from  $n = 40$  that were selected ( $p = 2.3 \text{ E-}20$  to  $7.0 \text{ E-}11$ ). It is assumed, that single or multiple categorical values, as indicated in Biobank, are similarly processed and results would suggest that caveolin-1/2 variants have a population-wide effect. That result has to be compared to the impact of the over 100 human genes with variants suggested to play a role (Roselli et al. 2018) and would be an interesting study in itself.

Putative genetic evidence for a causal association of blood pressure and atrial fibrillation and flutter, a relation that is described in medical statistics, is provided in Fig. 4 B. MR (Mendelian Randomization) Egger regression with MR-Base (Hemani et al. 2018) and other tests were used to demonstrate the link by using SNPs of several studies with 46 and 94 SNPs in the exposure and outcome group, respectively, using the SNP pruning option due to linkage disequilibrium. The  $p = 0.02$  suggests that the sample size should, yet, be elevated to clearly demonstrate the small beta with little intercept value.

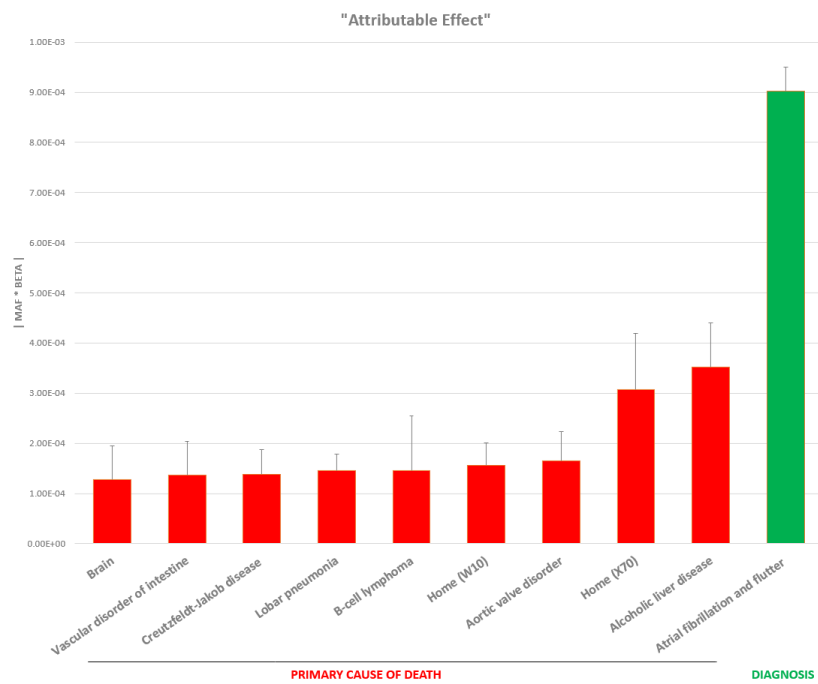


**Fig. 4 A The Population Attributable Score**

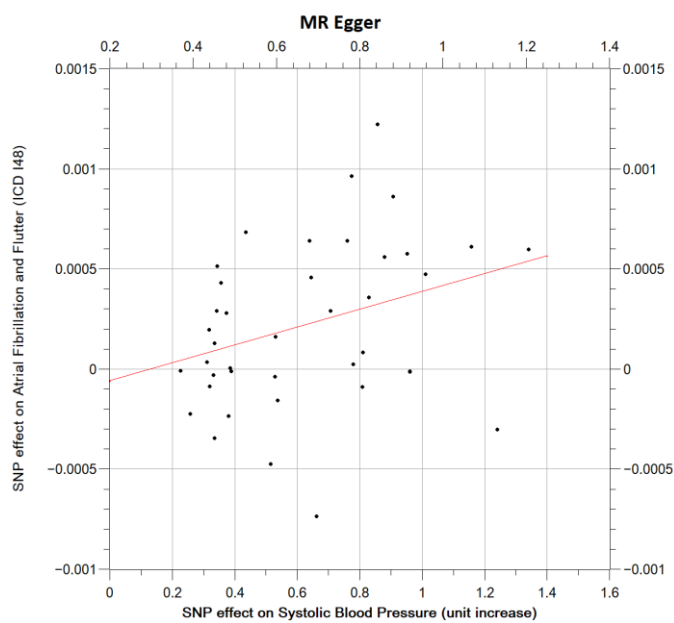


**Fig. 4 B Genetic Evidence for an Association**







**Fig. 4 E Top Scoring IMEX-GO Terms**

Tentative Assignment of Gene Ontology Terms to the Retrieved Protein Network (PSICQUIC) from UK Biobank I48 Entries: Atrial Fibrillation and Flutter

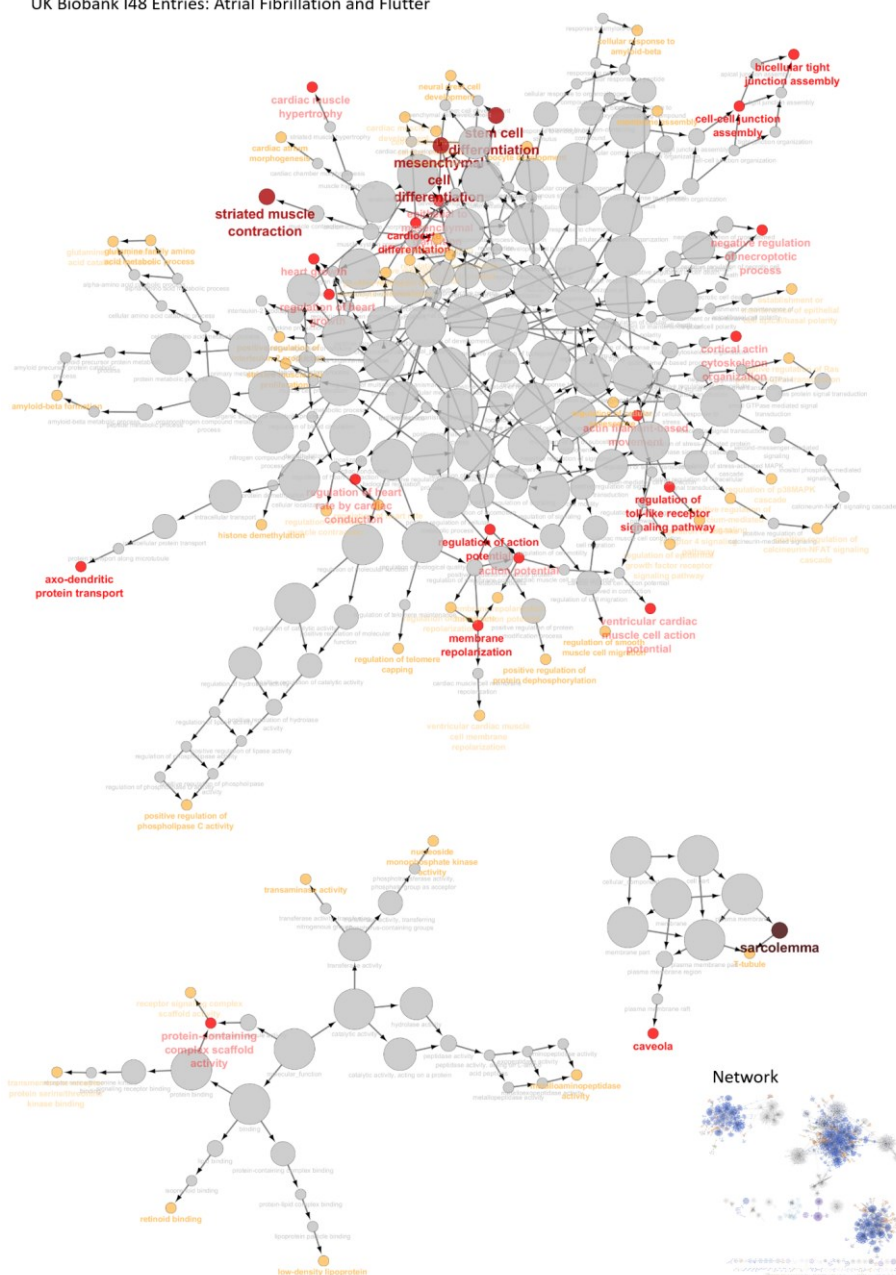


**Fig. 4 F GO Terms of Protein Network “Fibrillation and Flutter”**

**Figure 4: Genetics and System-Wide Interactome of Atrial Fibrillation and Blood Pressure.** The population attributable score (A) (similar to relative risk versus attributable risk) can be generated from UK Biobank data, and confirms recent genetic evidence that Cav1 is involved in forming a risk (benefit at higher expression levels) for atrial fibrillation and flutter from GWAS results (rs55883210 and linked rs10271007). Top 10 scores are shown from  $n = 40$  that were selected ( $p = 2.3 \times 10^{-20}$  to  $7.0 \times 10^{-11}$ ). Putative genetic evidence for a causal association of blood pressure and atrial fibrillation and flutter (B). MR (Mendelian Randomization) Egger regression with MR-Base and other tests were used to demonstrate the link by using SNPs of several studies with 46 and 94 SNPs in the exposure and outcome group, respectively, using the SNP pruning option due to linkage disequilibrium. Number of cases 5669 and controls 457341 showed the  $p=0.02$ , the sample size should, yet, be elevated to clearly demonstrate the small beta with little intercept value (see MR-Base from <http://www.mrbase.org>) (Hemani et al. 2018). Network for ICD10 I48 and Systolic Blood Pressure from PSICQUIC (IMEX data: ClueGO graph) with important nodes (C). The gene ontology (GO) of the protein-protein etc. interaction network includes 7712 terms in the complete listing from *Homo sapiens* (D). In this network, the top-scoring 45 GO-Terms (P-Value) were evaluated for gene occurrence and listed in this simple wordle style (E). (F) Tentative Assignment of Gene Ontology Terms to the Retrieved Protein Network (PSICQUIC) from UK Biobank I48 Entries: Atrial Fibrillation and Flutter.

The network for ICD10 I48 (Atrial Fibrillation and Flutter) and Systolic Blood Pressure was graphed from PSICQUIC with important nodes (Fig. 4 C). Next to caveolar roles, a multitude of physiological functions have been found to be associated evaluating biochemical data as shown here. Heart morphogenesis, cardiocyte differentiation, muscle contraction and regulation of protein phosphorylation are just some of the terms that are important. The gene ontology (GO) of the protein-protein etc. interaction network includes 7712 terms in the complete listing from *Homo sapiens* (Fig. 4 D) and is shown as an overview. In this network, the top-scoring 45 GO-Terms (P-Value) were evaluated for gene occurrence and listed also in this simple wordle style (Fig. 4 E). Several good reviews have recently come to similar conclusions. As a further test to provide insight to the complex network of proteins and regulation in atrial fibrillation only (Fig. 4 F) the gene ontology terms were assigned to the protein network (PSICQUIC) from UK Biobank I48 entries. This network alone is listing the most important functions that range from intercellular tight-junction assembly, mesenchymal and stem cell differentiation, axo-dendritic protein transport, membrane repolarization and regulation of the toll-like receptor signaling among other functions. Caveolae and a relation to T-tubules and the sarcolemma are also indicated.

SNP	Pos (hg19)	A1*	A2*	Trait	Source	Beta	P	N
rs55883210	chr7:116160524	A	G	Atrial fibrillation and flutter	UKBB	0.001898	1.82e-13	337199
rs10271007	chr7:116145849	A	G	Atrial fibrillation and flutter	UKBB	-0.001840	9.36e-13	337199
rs10271007	chr7:116145849	A	G	Systolic blood pressure	UKBB	0.011700	2.00e-06	317754
rs55883210	chr7:116160524	A	G	Systolic blood pressure	UKBB	-0.011520	2.93e-06	317754
rs55883210	chr7:116160524	A	G	Self-reported atrial fibrillation	UKBB	0.001001	3.33e-06	337159
rs10271007	chr7:116145849	A	G	Self-reported atrial fibrillation	UKBB	-0.000961	8.04e-06	337159

\* The minor allele is reflected in A1 in one and A2 in the other SNP, the effect of each is similar; modified from PhenoScanner (Staley et al. 2016).

**Table 1: Traits in Cav2/Cav1 SNPs.** The caveolin SNPs shown here do not follow the MR Egger trend, by demonstrating increased systolic blood pressure and lower observed atrial fibrillation. Altered lipoprotein-profiles discovered in cav1 -/- mice had not been confirmed in current GWAS data.

Caveolin-1 in cell cultures of primary type may seldomly localize to mature focal adhesions

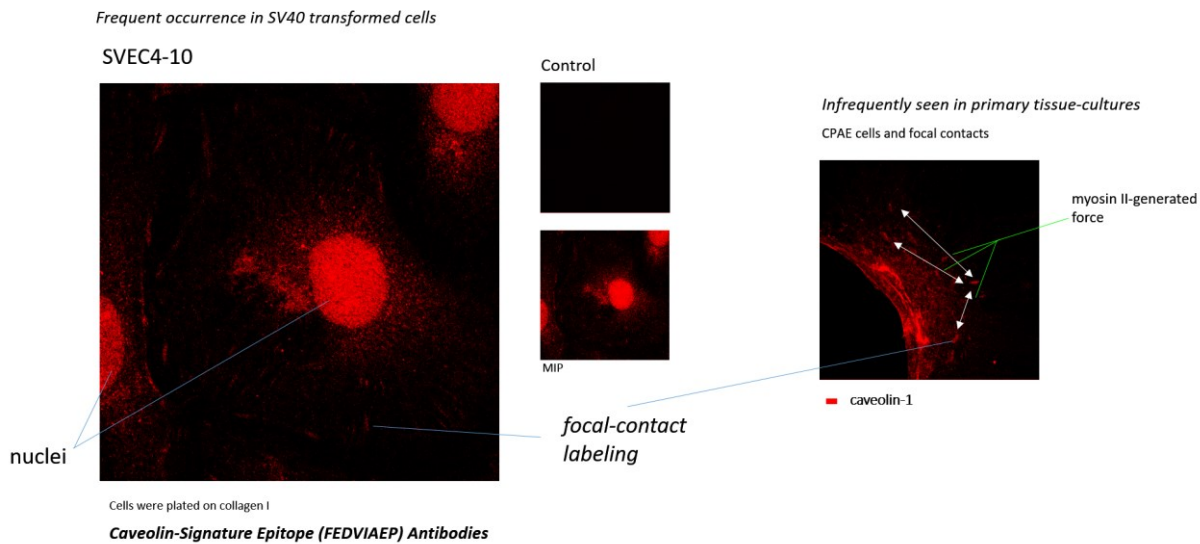


Fig. 5 A Caveolae in Transformed and Primary Cultured Cells

The interplay of caveolae and maturation of focal contacts has not been clarified but may include membrane- as well as protein turnover

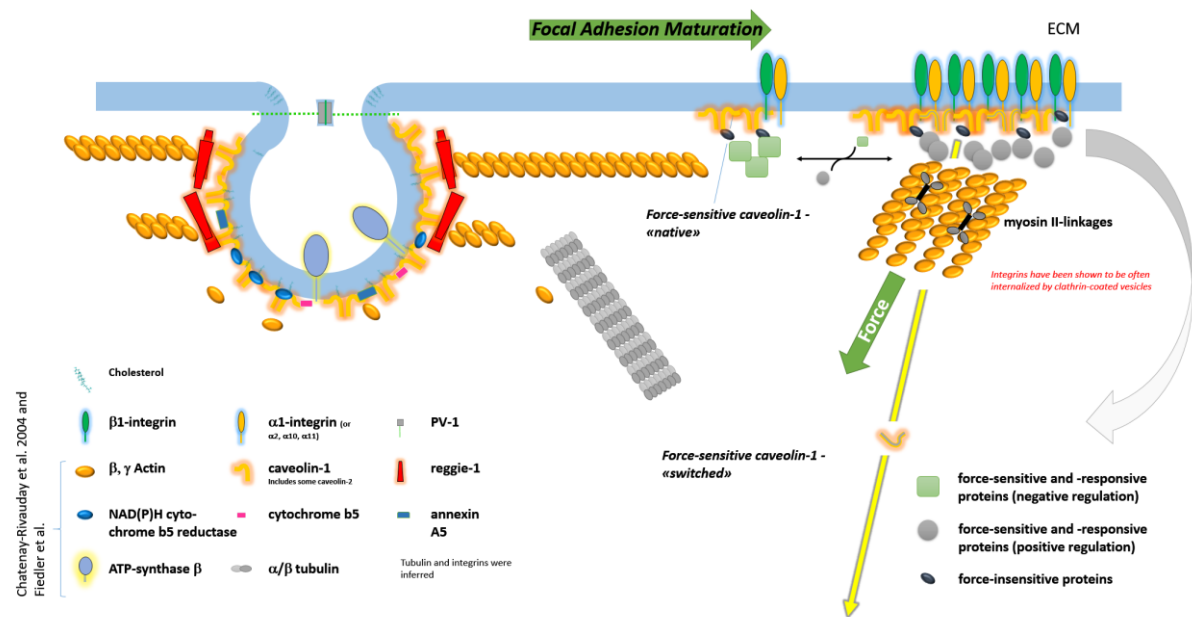


Fig. 5 B Caveolae and Role of Integrins

# Integrin codes are redescribed in the expression analysis

See  $\alpha 1$ ,  $\alpha 2$ ,  $\alpha 5$ ,  $\alpha 6$ ,  $\alpha 9$ ,  $\alpha v$ ,  $\beta 1$  high for the arterial endothelial trajectory

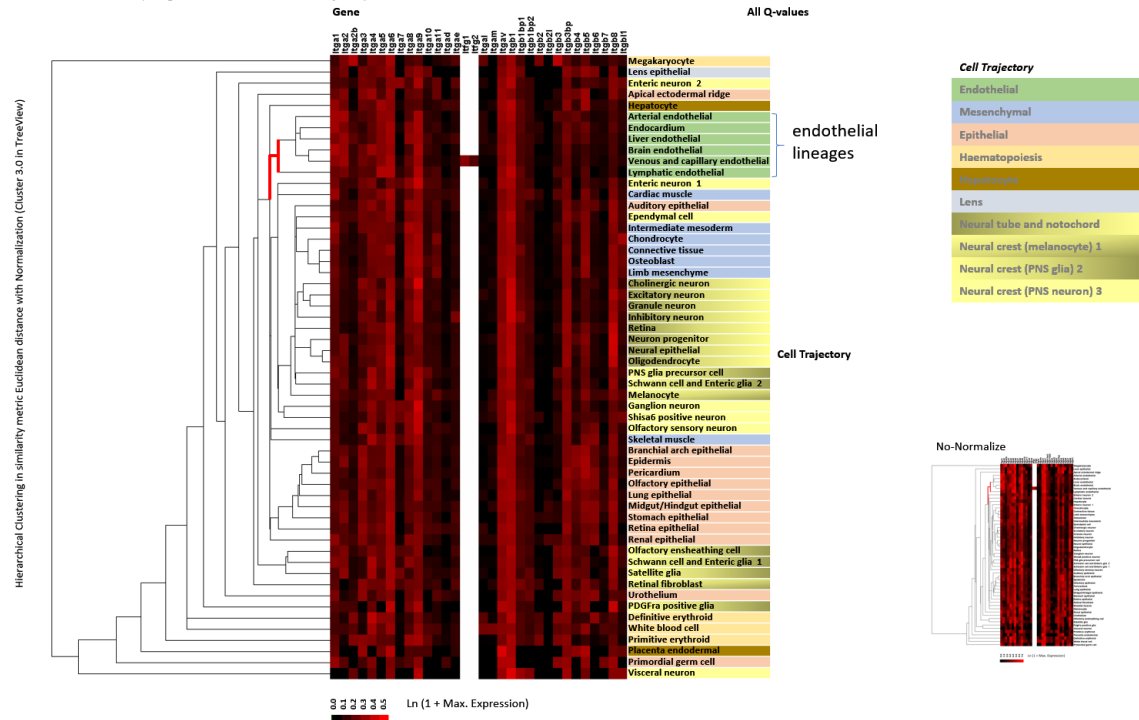


Fig. 5 C Integrin Code

Transcytosis follows a major route that had not been considered by supporters of the caveolae- «vesicle-transcytosis»

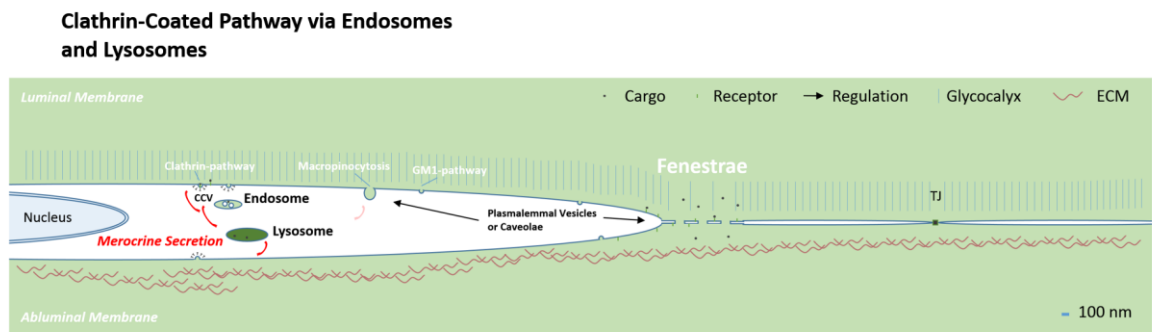


Fig. 5 D Transcytosis Follows Several Routes

**Figure 5: Role of caveolae in cell migration.** Early indications on the role of caveolin-1 in integrin functions (Wary et al. 1996) (A) have been confirmed in transformed cultured and partially confirmed in primary cultured mammalian cell types. The antibodies against the caveolin-1 “signature-epitope” and 14 N-terminal caveolin-1 $\alpha$  residues, described in our reports (Chatenay-Rivauday et al. 2004; Kuzmenko et al. 2004), were used for labelling of primary cultured cells (CPAE, calf pulmonary



artery endothelial cells) and transformed SVEC4-10 (mouse lymphoid endothelial) cells (O'Connell & Edidin 1990). **(B)** Force-responsive and force-sensitive proteins may be internalized at focal contacts: Model of caveolin internalization or endocytosis that contributes to caveolae turnover and is related to the cytoskeleton and focal contact maturations. The PV-1 protein of endothelial diaphragms was identified by Stan et al. as one of the first plasmalemmal (caveolae) proteins in addition to the marker caveolin-1 (Stan et al. 1999) and is shown at the diaphragm. **(C)** Integrins apparently form a "code" for different cell types. The grouping due to different integrin expression can be visualized with TreeView (<http://jtreeview.sourceforge.net>) in Cluster 3.0 (software package from M. de Hoon). Data were from Cao et al. (Cao et al. 2019). **(D)** Although the relationship of caveolae to transcytosis and endocytosis has been emphasized by several researchers, we had not found convincing evidence for a high-capacity exchange via caveolae across the endothelial cell layer. Current models predict a role of clathrin-coated vesicles in endocytosis coupled to bidirectional release of endocytosed proteins or envision macrophagocytic processes in the uptake of substances and release to the interstitium, the tissue side. We had also predicted, given the non-automatized tissue-culturing that was available back in 1998, that a diffusion pathway of substances coupled to a surface receptor, would allow exchange of materials across the cell layer. Kuzmenko et al. found, that the diffusion pathways could not outcompete the high-capacity endosomal transfer but were also not affected in a similar way by temperature (Kuzmenko et al. 2004). ECM: Extracellular matrix, TJ: Tight-junction.

Our discovery of Cav1 in the nucleus of transformed SVEC4-10 cells (mouse) may today be understood in the context of nuclear targeting or regulation upon known "conformational switching" of protein substrates upon force impact at matured focal adhesions, and regulation of transcription (see focal-contact type labeling **Fig. 5 A, Fig. 5 B**) (Kwon et al. 2011; Sanna et al. 2007). Interestingly, further evaluations have shown that focal adhesion integrins can be used to demonstrate the integrin codes by the latest study on expression levels. This study had been conducted with 56 mouse cell lineages which had been captured by single-cell RNA sequencing (**Fig. 5 C**) (Cao et al. 2019). The role of caveolin-1 established in integrin-signaling or -interaction would now pertain also to cell adhesion or even to the definition of cell identities. Endothelial cells can be grouped by hierarchical re-clustering into a lineage including 6 branches derived in this post-processing. The role of caveolae, implicated in tumor development, had been widely discussed and may be related to the signaling function and microenvironment in tumor tissues that may or may not be reproducible (Goetz et al. 2011; Sheen et al. 2019). A role in tumor suppression was described in transgenic mice (Williams et al. 2003), but a role as suppressor had also remained controversial and may be related to cell migration (Zhang et al. 2000).

Finally, the research in my laboratory has also shown that transcytosis in lymph vascular endothelia can occur by basic mechanisms such as membrane diffusion of receptors (Kuzmenko et al. 2004). This receptor-mediated pathway had not been described by other researchers in this area (**Fig. 5 D**), but would include routes that had previously been named "paracellular" transport via junctions or fenestrae. Indeed, one or several trans-endothelial routes (via lysosomes) described in this work may today be used as clinically important transvascular treatment pathways (Johnsen et al. 2017).



### Local and Metabolic Effects



32567 cells included in evaluation

\* Madcam1<sup>+</sup> cells EDL: M. extensor digitorum longus Muscle: EDL + M. soleus  
interferon: interferon-activated with markers angiogenic (with markers)

## Proposed function of encoded proteins in cells of blood vascular endothelia

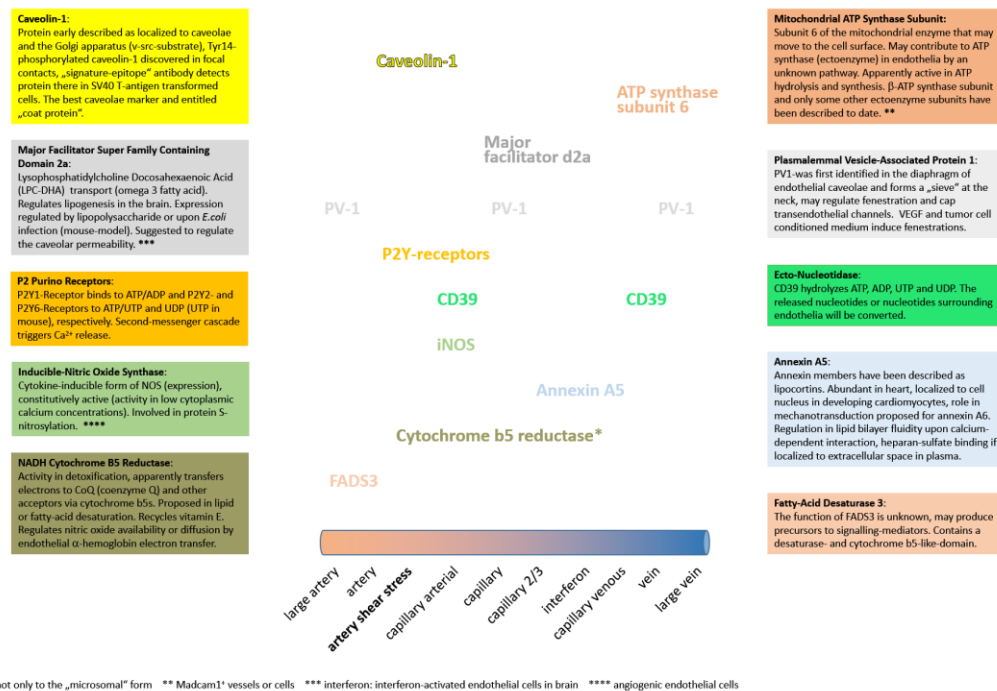


**Fig. 6 C Functions in Endothelia**

**Figure 6: Outlook on caveolae role.** (A) The proteome of caveolae from lung endothelia of *R. norvegicus* suggested to us, that few very abundant proteins would be found in addition to the coat protein caveolin-1. Only reggie-1/flotillin-2 (Volonte et al. 1999) was found as a major second component. Functions that include HDL binding of ATP synthase, the ectoenzyme likely found in caveolae and localized to the plasma membrane, and further signaling mechanisms involving ATP and  $Ca^{2+}$  are indicated. The NO signaling pathway found by Straub et al. (Straub et al. 2012) and likely related to our finding of cytochrome b5 reductase (Cyb5R3) bound to caveolin-1 is presented and drawn in the inset. Tensegrity of the cells and signaling across the layer is described and may related to caveolin in focal contacts or caveolae themselves. (B) Specialization of different endothelial cell types has recently been analyzed. The single-cell RNA sequencing resulted in the surprising discovery of (at least) 12 cell sub-groups with one "artery shear stress" and NADH cytochrome b5 reductase and the P2Y2-receptor as cellular markers in brain (Kalucka et al. 2020). Fatty-acid desaturase (FADS3) was for example found in muscle and lung in arteries. Other examples of top 50 markers found include Cav1 (testis and liver), MT-ATP6 (small intestine Madcam1<sup>+</sup> cells), Mfsd2a (testis and brain), PLVAP (PV-1; small intestine, liver, lung, kidney, heart and extensor digitorum longus / soleus musculi and testis), P2ry1 (brain and kidney glomeruli), P2ry6 (small intestine), Entpd1 (small intestine, heart, liver and musculus extensor digitorum longus), NOS2 ((angiogenic) kidney), Anxa1 (heart), Anxa5 (spleen), Cyb5r3 (brain, colon and testis) and also Cyb5a (testis). (C) Known functions of indicated proteins are listed and discussed in relation to the results of Kalucka et al. (Kalucka et al. 2020).

## Views on caveolae

A current view on the caveolae signaling that may prevail in many vascular beds is summarized in this overview (Fig. 6 A). The role of NADH-cytochrome b5 reductase (Cyb5R3) in vasosignaling was begun to be clarified in the last years (Straub et al. 2012). Likely pulmonary hypertension in lung involves the same signaling mechanisms and it may implicate caveolae in this signaling axis (Alvarez et al. 2017). Neurovascular coupling, that could involve lipids and has recently been demonstrated in brain arteriolar vessels in mice, is shown to be also independent of endothelial nitric oxide synthase (eNOS)

and required, you may have guessed, Cav1 ([Chow et al. 2020](#)). Our biochemical analysis not only provided an idea on the proteins involved in vasocoupling, but also the recent single-cell RNA sequencing analysis (**Fig. 6 B, Fig. 6 C**) ([Kalucka et al. 2020](#)). Here, the top 50 class of markers for the defined shear stress arteries included the Cyb5R3 protein. The knowledge on details of assembly of the supramolecular complex of eNOS, Cav1, Cyb5R3 and  $\alpha$ -hemoglobin and its enzymology require further interesting studies i.e. on electron-transfer mechanisms. The enigmatic circumstance, that eNOS is proposed to involve  $1\frac{1}{2}$  NADPH molecules in NO synthesis and implicates inter-protomer as well as inter-domain electron transfer, and a new supermolecular pathway of Cyb5R3-derived "electron channeling" in the nitrate pathway, could be integrated into the overall scheme of the reaction. Not all caveolae may be active in a particular, pre-determined signaling pathway. Finally, a recent whole exome sequence analysis speaks for the role of caveolae and caveolins (Cav1/Cav2) in (for the coding DNA region) diastolic blood pressure, systolic (brachial) blood pressure, pulse rate, electrocardiogram phase time, and HDL cholesterol among other health parameters and inferred phenotypes that have been studied ([Cirulli & Washington 2019](#)). Today's knowledge on presumed cytoplasmic oscillators that may couple to signaling reactions, and tissue behavior that is determined by autocrine, paracrine and junctional signal transmission that may lead to bifurcations in single cell behaviors, necessitates single cell analyses before the elucidated composite sequence and order of molecular reactions can be firmly established.

## References

- Adam, G., & Delbrück, M. (1968). Reduction of dimensionality in biological diffusion processes. In A. Rich & N. Davidson (Eds.), *Structural chemistry and molecular biology* (pp. 198–215). W.H. Freeman.
- Alvarez, R. A., Miller, M. P., Hahn, S. A., Galley, J. C., Bauer, E., Bachman, T., Hu, J., Sembrat, J., Goncharov, D., Mora, A. L., Rojas, M., Goncharova, E., & Straub, A. C. (2017). Targeting pulmonary endothelial hemoglobin alpha improves nitric oxide signaling and reverses pulmonary artery endothelial dysfunction. *American Journal of Respiratory Cell and Molecular Biology*, 57(6), 733–744. DOI [10.1165/rcmb.2016-0418OC](https://doi.org/10.1165/rcmb.2016-0418OC)
- Anderson, D. H., Kickhoefer, V. A., Sievers, S. A., Rome, L. H., & Eisenberg, D. (2007). Draft crystal structure of the vault shell at 9-Å resolution. *PLoS Biology*, 5(11), e318. DOI [10.1371/journal.pbio.0050318](https://doi.org/10.1371/journal.pbio.0050318)
- Andreone, B. J., Chow, B. W., Tata, A., Lacoste, B., Ben-Zvi, A., Bullock, K., Deik, A. A., Ginty, D. D., Clish, C. B., & Gu, C. (2017). Blood-brain barrier permeability is regulated by lipid transport-dependent suppression of caveolae-mediated transcytosis. *Neuron*, 94(3), 581–594. DOI [10.1016/j.neuron.2017.03.043](https://doi.org/10.1016/j.neuron.2017.03.043)
- Astudillo, A. M., Perez-Chacon, G., Meana, C., Balgoma, D., Pol, A., Del Pozo, M. A., Balboa, M. A., & Balsinde, J. (2011). Altered arachidonate distribution in macrophages from caveolin-1 null mice leading to reduced eicosanoid synthesis. *The Journal of Biological Chemistry*, 286(40), 35299–35307. DOI [10.1074/jbc.M111.277137](https://doi.org/10.1074/jbc.M111.277137)
- Balsinde, J., Balboa, M., & Dennis, E. (1998). Functional coupling between secretory phospholipase A2 and cyclooxygenase-2 and its regulation by cytosolic group IV phospholipase A2. *Proceedings of The National Academy Of Sciences*, 95, 7951–7956. DOI [10.1073/pnas.95.14.7951](https://doi.org/10.1073/pnas.95.14.7951)
- Blanchard, H., Boulier-Monthéan, N., Legrand, P., & Pédrone, F. (2014). The 51kDa fatty acid desaturase 3 (FADS3) is not microsomal but secreted in the extracellular matrix of hepatocytes and blood in rat. *Journal of Cellular Biochemistry*, 115(1), 199–207. DOI [10.1002/jcb.24651](https://doi.org/10.1002/jcb.24651)
- Bousserouel, S., Brouillet, A., Béréziat, G., Raymondjean, M., Andréani, M., Physiologie, U. M. R., Pierre, U., Bâtiment, A., Bernard, S., & Cedex, P. (2003). Different effects of n-6 and n-3 polyunsaturated fatty acids on the activation of rat smooth muscle cells by interleukin-1 $\beta$ . *Journal of Lipid Research*, 44, 601–611. DOI [10.1194/jlr.M200092-JLR200](https://doi.org/10.1194/jlr.M200092-JLR200)
- Bruschi, M., Santucci, L., Ravera, S., Candiano, G., Bartolucci, M., Calzia, D., Lavarello, C., Inglese, E., Ramenghi, L. A., Petretto, A., Ghiggeri, G. M., & Panfoli, I. (2016). Human urinary exosome proteome unveils its aerobic respiratory ability. *Journal of Proteomics*, 136, 25–34. DOI [10.1016/j.jprot.2016.02.001](https://doi.org/10.1016/j.jprot.2016.02.001)
- Cao, J., Spielmann, M., Qiu, X., Huang, X., Ibrahim, D. M., Hill, A. J., Zhang, F., Mundlos, S., Christiansen, L., Steemers, F. J., Trapnell, C., & Shendure, J. (2019). The single-cell transcriptional landscape of mammalian organogenesis. *Nature*, 566(7745), 496–502. DOI [10.1038/s41586-019-0969-x](https://doi.org/10.1038/s41586-019-0969-x)
- Chatenay-Rivauday, C., Cakar, P., Jenö, P., Kuzmenko, E. S., & Fiedler, K. (2004). Caveolae: Biochemical analysis. *Molecular Biology Reports*, 31, 67–84. DOI [10.1023/B:MOLE.0000031352.51910.e9](https://doi.org/10.1023/B:MOLE.0000031352.51910.e9)

- Chow, B. W., Nuñez, V., Kaplan, L., Granger, A. J., Bistrong, K., Zucker, H. L., Kumar, P., Sabatini, B. L., & Gu, C. (2020). Caveolae in CNS arterioles mediate neurovascular coupling. *Nature*, 579, 106–110. DOI [10.1038/s41586-020-2026-1](https://doi.org/10.1038/s41586-020-2026-1)
- Cirulli, E., & Washington, N. (2019). UK Biobank. Exome rare variant analysis. In *Helix Research*. <https://blog.helix.com/uk-biobank-helix-research/>.
- Das, K., Lewis, R. Y., Scherer, P. E., & Lisanti, M. P. (1999). The membrane-spanning domains of caveolins-1 and-2 mediate the formation of caveolin hetero-oligomers - Implications for the assembly of caveolae membranes in vivo. *Journal of Biological Chemistry*, 274(26), 18721–18728. DOI [10.1074/jbc.274.26.18721](https://doi.org/10.1074/jbc.274.26.18721)
- Deng, X., Morris, J., Dressmen, J., Tubb, M., Tso, P., Jerome, W., Davidson, W., & Thompson, T. (2012). The Structure of Dimeric Apolipoprotein A-IV and Its Mechanism of Self-Association. *Structure*, 20, 767–779. DOI [10.1016/j.str.2012.02.020](https://doi.org/10.1016/j.str.2012.02.020)
- Drab, M., Verkade, P., Elger, M., Kasper, M., Lohn, M., Lauterbach, B., Menne, J., Lindschau, C., Mende, F., Luft, F. C., Schedl, A., Haller, H., & Kurzchalia, T. V. (2001). Loss of caveolae, vascular dysfunction and pulmonary defects in caveolin-1 gene-disrupted mice. *Science*, 293, 2449–2452. DOI [10.1126/science.1062688](https://doi.org/10.1126/science.1062688)
- Ellinor, P. T., Lunetta, K. L., Albert, C. M., Glazer, N. L., Ritchie, M. D., Smith, A. V., Arking, D. E., Müller-Nurasyid, M., Krijthe, B. P., Lubitz, S. a, Bis, J. C., Chung, M. K., Dörr, M., Ozaki, K., Roberts, J. D., Smith, J. G., Pfeufer, A., Sinner, M. F., Lohman, K., ... Kääb, S. (2012). Meta-analysis identifies six new susceptibility loci for atrial fibrillation. *Nature Genetics*, 44(6), 670–675. DOI [10.1038/ng.2261](https://doi.org/10.1038/ng.2261)
- Fernandez, I., Ying, Y., Albanesi, J., & Anderson, R. G. W. (2002). Mechanism of caveolin filament assembly. *Proceedings of the National Academy of Sciences*, 99(17), 11193–11198. DOI [10.1073/pnas.172196599](https://doi.org/10.1073/pnas.172196599)
- Fiedler, K. (2002). Caveolae in mechanotransduction. *Mol. Biol. Cell Suppl.*, 13, 232a.
- Fiedler, K. (2008a). Caveolin-1 is similar to the regulatory loop and lipid binding core of the P1TP  $\alpha$ . In [klausfiedler.ch](http://klausfiedler.ch). <https://www.klausfiedler.ch/cav1pitp.pdf>.
- Fiedler, K. (2008b). The clathrin and a caveolar coat may assemble similarly. In [klausfiedler.ch](http://klausfiedler.ch). [https://www.klausfiedler.ch/Caveolae\\_Coat\\_Reggie\\_Flotillin.pdf](https://www.klausfiedler.ch/Caveolae_Coat_Reggie_Flotillin.pdf).
- Fiedler, K. (2012). Biochemical Analysis of Caveolae. In [klausfiedler.ch](http://klausfiedler.ch). <https://www.klausfiedler.ch/Biozentrum.html>.
- Fiedler, K. (2018). The caveolin model. In [klausfiedler.ch](http://klausfiedler.ch). [https://www.klausfiedler.ch/CaveolinModel\\_Fiedler.pdf](https://www.klausfiedler.ch/CaveolinModel_Fiedler.pdf).
- Fielding, C. J., & Fielding, P. E. (2000). Cholesterol and caveolae: Structural and functional relationships. *Bba Mol Cell Biol Lipids*, 1529(1-3), 210–222. DOI [10.1016/s1388-1981\(00\)00150-5](https://doi.org/10.1016/s1388-1981(00)00150-5)
- Fiser, A., & Sali, A. (2003). Modeller: Generation and refinement of homology-based protein structure models. *Methods in Enzymology*, 374, 461–491. DOI [10.1016/S0076-6879\(03\)74020-8](https://doi.org/10.1016/S0076-6879(03)74020-8)
- García-Fernández, E., Koch, G., Wagner, R. M., Fekete, A., Stengel, S. T., Schneider, J., Mielich-Süss, B., Geibel, S., Markert, S. M., Stigloher, C., & Lopez, D. (2017). Membrane Microdomain Disassembly Inhibits MRSA Antibiotic Resistance. *Cell*, 171(6), 1354–1367.e20. DOI [10.1016/j.cell.2017.10.012](https://doi.org/10.1016/j.cell.2017.10.012)
- Glenney, J. R., & Soppet, D. (1992). Sequence and expression of caveolin, a protein component of caveolae plasma mebrane domains phosphorylated on tyrosine in Rous sarcoma virus-transformed fibroblasts. *Proceedings of the National Academy of Sciences*, 89(21), 10517–10521. DOI [10.1073/pnas.89.21.10517](https://doi.org/10.1073/pnas.89.21.10517)

- Goetz, J. G., Minguet, S., Navarro-Lérida, I., Lazcano, J. J., Samaniego, R., Calvo, E., Tello, M., Osteso-Ibáñez, T., Pellinen, T., Echarri, A., Cerezo, A., Klein-Szanto, A. J. P., Garcia, R., Keely, P. J., Sánchez-Mateos, P., Cukierman, E., & Del Pozo, M. A. (2011). Biomechanical Remodeling of the Microenvironment by Stromal Caveolin-1 Favors Tumor Invasion and Metastasis. *Cell*, 146(1), 148–163. DOI [10.1016/j.cell.2011.05.040](https://doi.org/10.1016/j.cell.2011.05.040)
- Hayer, A., Stoeber, M., Ritz, D., Engel, S., Meyer, H. H., & Helenius, A. (2010). Caveolin-1 is ubiquitinated and targeted to intraluminal vesicles in endolysosomes for degradation. *The Journal of Cell Biology*, 191(3), 615–629. DOI [10.1083/jcb.201003086](https://doi.org/10.1083/jcb.201003086)
- Hemani, G., Zheng, J., Elsworth, B., Wade, K. H., Haberland, V., Baird, D., Laurin, C., Burgess, S., Bowden, J., Langdon, R., Tan, V. Y., Yarmolinsky, J., Shihab, H. A., Timpson, N. J., Evans, D. M., Relton, C., Martin, R. M., Davey Smith, G., Gaunt, T. R., & Haycock, P. C. (2018). The MR-Base platform supports systematic causal inference across the human phenome. *eLife*, 7. DOI [10.7554/elife.34408](https://doi.org/10.7554/elife.34408)
- Hill, M. M., Bastiani, M., Luetterforst, R., Kirkham, M., Kirkham, A., Nixon, S. J., Walser, P., Abankwa, D., Oorschot, V. M. J., Martin, S., Hancock, J. F., & Parton, R. G. (2008). PTRF-Cavin, a conserved cytoplasmic protein required for Caveola formation and function. *Cell*, 132(1), 113–124. DOI [10.1016/j.cell.2007.11.042](https://doi.org/10.1016/j.cell.2007.11.042)
- Hill, M. M., Daud, N. H., Aung, C. S., Loo, D., Martin, S., Murphy, S., Black, D. M., Barry, R., Simpson, F., Liu, L., Pilch, P. F., Hancock, J. F., Parat, M. O., & Parton, R. G. (2012). Co-regulation of cell polarization and migration by caveolar proteins PTRF/Cavin-1 and caveolin-1. *PLoS One*, 7(8), e43041. DOI [10.1371/journal.pone.0043041](https://doi.org/10.1371/journal.pone.0043041)
- Holm, H., Gudbjartsson, D. F., Arnar, D. O., Thorleifsson, G., Thorgeirsson, G., Stefansdottir, H., Gudjonsson, S. A., Jonasdottir, A., Mathiesen, E. B., Njolstad, I., Nyrnes, A., Wilsgaard, T., Hald, E. M., Hveem, K., Stoltenberg, C., Lochen, M.-L., Kong, A., Thorsteinsdottir, U., & Stefansson, K. (2010). Several common variants modulate heart rate, PR interval and QRS duration. *Nature Genetics*, 42(2), 117–122. DOI [10.1038/ng.511](https://doi.org/10.1038/ng.511)
- Hoop, C. L., Sivanandam, V. N., Kodali, R., Srnec, M. N., & Van der Wel, P. C. A. (2012). Structural characterization of the caveolin scaffolding domain in association with cholesterol-rich membranes. *Biochemistry*, 51(1), 90–99. DOI [10.1021/bi201356v](https://doi.org/10.1021/bi201356v)
- Hubert, M., Larsson, E., Vegesna, N. V. G., Ahnlund, M., Johansson, A. I., Moodie, L. W., & Lundmark, R. (2020). Lipid accumulation controls the balance between surface connection and scission of caveolae. *eLife*, 9. DOI [10.7554/elife.55038](https://doi.org/10.7554/elife.55038)
- Johnsen, K. B., Burkhart, A., Melander, F., Kempen, P. J., Vejlebo, J. B., Siupka, P., Nielsen, M. S., Andresen, T. L., & Moos, T. (2017). Targeting transferrin receptors at the blood-brain barrier improves the uptake of immunoliposomes and subsequent cargo transport into the brain parenchyma. *Scientific Reports*, 7(1), 10396. DOI [10.1038/s41598-017-11220-1](https://doi.org/10.1038/s41598-017-11220-1)
- Kalucka, J., de Rooij, L. P. M. H., Goveia, J., Rohlenova, K., Dumas, S. J., Meta, E., Conchinha, N. V., Taverna, F., Teuwen, L.-A., Veys, K., García-Caballero, M., Khan, S., Geldhof, V., Sokol, L., Chen, R., Treps, L., Borri, M., de Zeeuw, P., Dubois, C., ... Carmeliet, P. (2020). Single-cell transcriptome atlas of murine endothelial cells. *Cell*, 180(4), 764–779.e20. DOI [10.1016/j.cell.2020.01.015](https://doi.org/10.1016/j.cell.2020.01.015)
- Khater, I. M., Meng, F., Wong, T. H., Nabi, I. R., & Hamarneh, G. (2018). Super resolution network analysis defines the molecular architecture of caveolae and caveolin-1 scaffolds. *Scientific Reports*, 8(1), 9009. DOI [10.1038/s41598-018-27216-4](https://doi.org/10.1038/s41598-018-27216-4)



- Kuzmenko, E. S., Djafarzadeh, S., Cakar, Z. P., & Fiedler, K. (2004). LDL transcytosis by protein membrane diffusion. *The International Journal of Biochemistry & Cell Biology*, 36(3), 519–534. DOI [10.1016/j.biocel.2003.09.010](https://doi.org/10.1016/j.biocel.2003.09.010)
- Kwon, H., Jeong, K., Hwang, E. M., Park, J.-Y., & Pak, Y. (2011). A novel domain of caveolin-2 that controls nuclear targeting: Regulation of insulin-specific ERK activation and nuclear translocation by caveolin-2. *Journal of Cellular and Molecular Medicine*, 15(4), 888–908. DOI [10.1111/j.1582-4934.2010.01079.x](https://doi.org/10.1111/j.1582-4934.2010.01079.x)
- Le Lay, S., Li, Q., Proschogo, N., Rodriguez, M., Gunaratnam, K., Cartland, S., Rentero, C., Jessup, W., Mitchell, T., & Gaus, K. (2009). Caveolin-1-dependent and -independent membrane domains. *Journal of Lipid Research*, 50(8), 1609–1620. DOI [10.1194/jlr.M800601-JLR200](https://doi.org/10.1194/jlr.M800601-JLR200)
- Liu, P. S., Li, W. P., Machleidt, T., & Anderson, R. G. W. (1999). Identification of caveolin-1 in lipoprotein particles secreted by exocrine cells. *Nature Cell Biology*, 1(6), 369–375. DOI [10.1038/14067](https://doi.org/10.1038/14067)
- Ludwig, A., Otto, G. P., Riento, K., Hams, E., Fallon, P. G., & Nichols, B. J. (2010). Flotillin microdomains interact with the cortical cytoskeleton to control uropod formation and neutrophil recruitment. *Journal of Cell Biology*, 191(4), 771–781. DOI [10.1083/jcb.201005140](https://doi.org/10.1083/jcb.201005140)
- Martinez, L. O., Jacquet, S., Esteve, J. P., Rolland, C., Cabezon, E., Champagne, E., Pineau, T., Georgeaud, V., Walker, J. E., Terce, F., Collet, X., Perret, B., & Barbaras, R. (2003). Ectopic beta-chain of ATP synthase is an apolipoprotein A-I receptor in hepatic HDL endocytosis. *Nature*, 421(6918), 75–79. DOI [10.1038/nature01250](https://doi.org/10.1038/nature01250)
- Monier, S., Dietzen, D. J., Hastings, W. R., Lublin, D. M., & Kurzchalia, T. V. (1996). Oligomerization of VIP21-caveolin in vitro is stabilized by long chain fatty acylation or cholesterol. *FEBS Letters*, 388(2-3), 143–149. DOI [10.1016/0014-5793\(96\)00519-4](https://doi.org/10.1016/0014-5793(96)00519-4)
- Moskowitz, I. P. G., Kim, J. B., Moore, M. L., Wolf, C. M., Peterson, M. A., Shendure, J., Nobrega, M. A., Yokota, Y., Berul, C., Izumo, S., Seidman, J. G., & Seidman, C. E. (2007). A molecular pathway including Id2, Tbx5, and Nkx2-5 required for cardiac conduction system development. *Cell*, 129(7), 1365–1376. DOI [10.1016/j.cell.2007.04.036](https://doi.org/10.1016/j.cell.2007.04.036)
- Murakami, M., Kambe, T., Shimbara, S., Yamamoto, S., Kuwata, H., & Kudo, I. (1999). Functional association of type IIA secretory phospholipase a 2 with the glycosylphosphatidylinositol-anchored heparan sulfate proteoglycan in the cyclooxygenase-2-mediated delayed prostanoid-biosynthetic pathway. *Journal of Biological Chemistry*, 274(42), 29927–29936. DOI [10.1074/jbc.274.42.29927](https://doi.org/10.1074/jbc.274.42.29927)
- Murakami, M., Sato, H., Miki, Y., Yamamoto, K., & Taketomi, Y. (2015). A new era of secreted phospholipase A2 (sPLA2). *Journal of Lipid Research*. DOI [10.1194/jlr.R058123](https://doi.org/10.1194/jlr.R058123)
- Müller-Marschhausen, K., Waschke, J., & Drenckhahn, D. (2008). Physiological hydrostatic pressure protects endothelial monolayer integrity. *American Journal of Physiology. Cell Physiology*, 294(1), C324–32. DOI [10.1152/ajpcell.00319.2007](https://doi.org/10.1152/ajpcell.00319.2007)
- O’Connell, K. A., & Edidin, M. (1990). A mouse lymphoid endothelial cell line immortalized by simian virus 40 binds lymphocytes and retains functional characteristics of normal endothelial cells. *Journal of Immunology*, 144, 521–525.
- Oh, P., & Schnitzer, J. E. (2001). Segregation of heterotrimeric G proteins in cell surface microdomains. G(q) binds caveolin to concentrate in caveolae, whereas G(i) and G(s) target lipid rafts by default. *Molecular Biology of the Cell*, 12(3), 685–698. DOI [10.1091/mbc.12.3.685](https://doi.org/10.1091/mbc.12.3.685)

- Osanai, T., Tanaka, M., Kamada, T., Nakano, T., Takahashi, K., Okada, S., Sirato, K., Magota, K., Kodama, S., & Okumura, K. (2001). Mitochondrial coupling factor 6 as a potent endogenous vasoconstrictor. *Journal of Clinical Investigation*, 108(7), 1023–30. DOI [10.1172/JCI11076](https://doi.org/10.1172/JCI11076)
- Ostermeyer, A. G., Ramcharan, L. T., Zeng, Y., Lublin, D. M., & Brown, D. A. (2004). Role of the hydrophobic domain in targeting caveolin-1 to lipid droplets. *The Journal of Cell Biology*, 164(1), 69–78. DOI [10.1083/jcb.200303037](https://doi.org/10.1083/jcb.200303037)
- Parker, B. L., Calkin, A. C., Seldin, M. M., Keating, M. F., Tarling, E. J., Yang, P., Moody, S. C., Liu, Y., Zerenturk, E. J., Needham, E. J., Miller, M. L., Clifford, B. L., Morand, P., Watt, M. J., Meex, R. C. R., Peng, K.-Y., Lee, R., Jayawardana, K., Pan, C., ... Drew, B. G. (2019). An integrative systems genetic analysis of mammalian lipid metabolism. *Nature*, 567(7747), 187–193. DOI [10.1038/s41586-019-0984-y](https://doi.org/10.1038/s41586-019-0984-y)
- Pelkmans, L., Kartenbeck, J., & Helenius, A. (2001). Caveolar endocytosis of simian virus 40 reveals a new two-step vesicular-transport pathway to the ER. *Nature Cell Biology*, 3(5), 473–483. DOI [10.1038/35074539](https://doi.org/10.1038/35074539)
- Raouf, R., Lolignier, S., Sexton, J. E., Millet, Q., Santana-Varela, S., Biller, A., Fuller, A. M., Pereira, V., Choudhary, J. S., Collins, M. O., Moss, S. E., Lewis, R., Tordo, J., Henckaerts, E., Linden, M., & Wood, J. N. (2018). Inhibition of somatosensory mechanotransduction by annexin A6. *Science Signaling*, 11(535). DOI [10.1126/scisignal.aao2060](https://doi.org/10.1126/scisignal.aao2060)
- Razani, B., Combs, T. P., Wang, X. B., Frank, P. G., Park, D. S., Russell, R. G., Li, M., Tang, B., Jelicks, L. A., Scherer, P. E., & Lisanti, M. P. (2002). Caveolin-1-deficient mice are lean, resistant to diet-induced obesity, and show hypertriglyceridemia with adipocyte abnormalities. *Journal of Biological Chemistry*, 277(10), 8635–8647. DOI [10.1074/jbc.M110970200](https://doi.org/10.1074/jbc.M110970200)
- Razani, B., & Lisanti, M. P. (2001). Caveolin-deficient mice: Insights into caveolar function human disease. *Journal of Clinical Investigation*, 108(11), 1553–1561. DOI [10.1172/JCI14611](https://doi.org/10.1172/JCI14611)
- Razani, B., Wang, X. B., Engelman, J. A., Battista, M., Lagaud, G., Zhang, X. L., Kneitz, B., Hou, H., Christ, G. J., Edelmann, W., & Lisanti, M. P. (2002). Caveolin-2-deficient mice show evidence of severe pulmonary dysfunction without disruption of caveolae. *Molecular and Cellular Biology*, 22(7), 2329–2344. DOI [10.1128/MCB.22.7.2329-2344.2002](https://doi.org/10.1128/MCB.22.7.2329-2344.2002)
- Riento, K., Zhang, Q., Clark, J., Begum, F., Stephens, E., Wakelam, M. J., & Nichols, B. J. (2018). Flotillin proteins recruit sphingosine to membranes and maintain cellular sphingosine-1-phosphate levels. *PLoS One*. DOI [10.1371/journal.pone.0197401](https://doi.org/10.1371/journal.pone.0197401)
- Roselli, C., Chaffin, M. D., Weng, L.-C., Aeschbacher, S., Ahlberg, G., Albert, C. M., Almgren, P., Alonso, A., Anderson, C. D., Aragam, K. G., Arking, D. E., Barnard, J., Bartz, T. M., Benjamin, E. J., Bihlmeyer, N. A., Bis, J. C., Bloom, H. L., Boerwinkle, E., Bottinger, E. B., ... Ellinor, P. T. (2018). Multi-ethnic genome-wide association study for atrial fibrillation. *Nature Genetics*, 50(9), 1225–1233. DOI [10.1038/s41588-018-0133-9](https://doi.org/10.1038/s41588-018-0133-9)
- Sando, J. J., & Chertihin, O. I. (1996). Activation of protein kinase C by lysophosphatidic acid: Dependence on composition of phospholipid vesicles. *The Biochemical Journal*, 317 ( Pt 2), 583–588. DOI [10.1042/bj3170583](https://doi.org/10.1042/bj3170583)
- Sanna, E., Miotti, S., Mazzi, M., De Santis, G., Canevari, S., & Tomassetti, A. (2007). Binding of nuclear caveolin-1 to promoter elements of growth-associated genes in ovarian carcinoma cells. *Experimental Cell Research*, 313(7), 1307–1317. DOI [10.1016/j.yexcr.2007.02.005](https://doi.org/10.1016/j.yexcr.2007.02.005)
- Schaum, N., Karkanas, J., Neff, N. F., May, A. P., Quake, S. R., Wyss-Coray, T., Darmanis, S., Batson, J., Botvinnik, O., Chen, M. B., Chen, S., Green, F., Jones, R. C., Maynard, A., Penland, L., Pisco, A. O., Sit, R. V., Stanley, G. M., Webber, J. T., ... Consortium, T. T. M. (2018). Single-cell

- transcriptomics of 20 mouse organs creates a Tabula Muris. *Nature*, 562(7727), 367–372. DOI [10.1038/s41586-018-0590-4](https://doi.org/10.1038/s41586-018-0590-4)
- Scheiffele, P., Verkade, P., Fra, A. M., Virta, H., Simons, K., & Ikonen, E. (1998). Caveolin-1 and -2 in the exocytic pathway of MDCK cells. *Journal of Cell Biology*, 140(4), 795–806. DOI [10.1083/jcb.140.4.795](https://doi.org/10.1083/jcb.140.4.795)
- Sheen, M. R., Fields, J. L., Northan, B., Lacoste, J., Ang, L.-H., & Fiering, S. (2019). Replication Study: Biomechanical remodeling of the microenvironment by stromal caveolin-1 favors tumor invasion and metastasis. *eLife*, 8. DOI [10.7554/eLife.45120](https://doi.org/10.7554/eLife.45120)
- Staley, J. R., Blackshaw, J., Kamat, M. A., Ellis, S., Surendran, P., Sun, B. B., Paul, D. S., Freitag, D., Burgess, S., Danesh, J., Young, R., & Butterworth, A. S. (2016). PhenoScanner: A database of human genotype-phenotype associations. *Bioinformatics (Oxford, England)*, 32(20), 3207–3209. DOI [10.1093/bioinformatics/btw373](https://doi.org/10.1093/bioinformatics/btw373)
- Stan, R. V., Kubitza, M., & Palade, G. E. (1999). PV-1 is a component of the fenestral and stomatal diaphragms in fenestrated endothelia. *Proceedings of the National Academy of Sciences*, 96(23), 13203–13207. DOI [10.1073/pnas.96.23.13203](https://doi.org/10.1073/pnas.96.23.13203)
- Stoeber, M., Schellenberger, P., Siebert, C. A., Leyrat, C., Helenius, A., & Grunewald, K. (2016). Model for the architecture of caveolae based on a flexible, net-like assembly of Cavin1 and Caveolin discs. *Proceedings of the National Academy of Sciences*, 113(50), E8069 LP–E8078. DOI [10.1073/pnas.1616838113](https://doi.org/10.1073/pnas.1616838113)
- Straub, A. C., Lohman, A. W., Billaud, M., Johnstone, S. R., Dwyer, S. T., Lee, M. Y., Bortz, P. S., Best, A. K., Columbus, L., Gaston, B., & Isakson, B. E. (2012). Endothelial cell expression of haemoglobin alpha regulates nitric oxide signalling. *Nature*, 491, 473. DOI [10.1038/nature11626](https://doi.org/10.1038/nature11626)
- Vatta, M., Ackerman, M. J., Ye, B., Makielski, J. C., Ughanze, E. E., Taylor, E. W., Tester, D. J., Balijepalli, R. C., Foell, J. D., Li, Z., Kamp, T. J., & Towbin, J. A. (2006). Mutant caveolin-3 induces persistent late sodium current and is associated with long-QT syndrome. *Circulation*, 114(20), 2104–2112. DOI [10.1161/CIRCULATIONAHA.106.635268](https://doi.org/10.1161/CIRCULATIONAHA.106.635268)
- Volonte, D., Galbiati, F., Li, S., Nishiyama, K., Okamoto, T., & Lisanti, M. P. (1999). Flotillins / cavatellins are differentially expressed in cells and tissues and form a hetero-oligomeric complex with caveolins in vivo. *Journal of Biological Chemistry*, 274(18), 12702–12709. DOI [10.1074/jbc.274.18.12702](https://doi.org/10.1074/jbc.274.18.12702)
- Wary, K. K., Mainiero, F., Isakoff, S. J., Marcantonio, E. E., & Giancotti, F. G. (1996). The adaptor protein shc couples a class of integrins to the control of cell cycle progression. *Cell*, 87, 733–743. DOI [10.1016/s0092-8674\(00\)81392-6](https://doi.org/10.1016/s0092-8674(00)81392-6)
- Waschke, J., Curry, F. E., Adamson, R. H., & Drenckhahn, D. (2004). Regulation of actin dynamics is critical for endothelial barrier functions. *American Journal of Physiology. Heart and Circulatory Physiology*. DOI [10.1152/ajpheart.00687.2004](https://doi.org/10.1152/ajpheart.00687.2004)
- Waschke, J., Golenhofen, N., Kurzchalia, T. V., & Drenckhahn, D. (2006). Protein kinase C-mediated endothelial barrier regulation is caveolin-1-dependent. *Histochemistry and Cell Biology*, 126(1), 17–26. DOI [10.1007/s00418-005-0140-7](https://doi.org/10.1007/s00418-005-0140-7)
- Whiteley, G., Collins, R. F., & Kitmitto, A. (2012). Characterization of the molecular architecture of human caveolin-3 and interaction with the skeletal muscle ryanodine receptor. *The Journal of Biological Chemistry*, 287(48), 40302–40316. DOI [10.1074/jbc.M112.377085](https://doi.org/10.1074/jbc.M112.377085)
- Willer, C. J., Schmidt, E. M., Sengupta, S., Peloso, G. M., Gustafsson, S., Kanoni, S., Ganna, A., Chen, J., Buchkovich, M. L., Mora, S., Beckmann, J. S., Bragg-Gresham, J. L., Chang, H.-Y., Demirkan, A., Den Hertog, H. M., Do, R., Donnelly, L. A., Ehret, G. B., Esko, T., ... Abecasis, G. R. (2013).

- Discovery and refinement of loci associated with lipid levels. *Nature Genetics*, 45(11), 1274–1283. DOI [10.1038/ng.2797](https://doi.org/10.1038/ng.2797)
- Williams, T. M., Cheung, M. W.-C., Park, D. S., Razani, B., Cohen, A. W., Muller, W. J., Di Vizio, D., Chopra, N. G., Pestell, R. G., & Lisanti, M. P. (2003). Loss of caveolin-1 gene expression accelerates the development of dysplastic mammary lesions in tumor-prone transgenic mice. *Molecular Biology of the Cell*, 14(3), 1027–1042. DOI [10.1091/mbc.e02-08-0503](https://doi.org/10.1091/mbc.e02-08-0503)
- Yamamoto, K., Shimizu, N., Obi, S., Kumagaya, S., Taketani, Y., Kamiya, A., & Ando, J. (2007). Involvement of cell surface ATP synthase in flow-induced ATP release by vascular endothelial cells. *American Journal of Physiology. Heart and Circulatory Physiology*, 293(3), H1646–1653. DOI [10.1152/ajpheart.01385.2006](https://doi.org/10.1152/ajpheart.01385.2006)
- Zhang, W., Razani, B., Altschuler, Y., Bouzahzah, B., Mostov, K. E., Pestell, R. G., & Lisanti, M. P. (2000). Caveolin-1 inhibits epidermal growth factor-stimulated lamellipod extension and cell migration in metastatic mammary adenocarcinoma cells (MTLn3) - Transformation suppressor effects of adenovirus-mediated gene delivery of caveolin-1. *Journal of Biological Chemistry*, 275(27), 20717–20725. DOI [10.1074/jbc.M909895199](https://doi.org/10.1074/jbc.M909895199)

**Supplement Linked**

[Supplementary Figure 1](#)

## Supplementary Table

Single-cell transcriptomics					
	cardioid-1	cardioid-2	cardioid-3	Pu010-1	Pu010-2
heart endothelial cell	0.22	0.26	0.01	0.75	0.66
limb endothelial cell	0.45	0.05	0	0.75	0.82
lung endothelial cell	0.22	0.26	0	1.21	0.96
brain pericyte	0.02	0.16	0.14	0.04	0.04
endothelial cell	0.02	0.1	0	1.38	1.54
fat endothelial cell	0.22	0.06	0.01	1.3	1.49
mammary endothelial cell	0.7	0.05	0.02	1.28	1.34
oligodendrocyte precursor cell	0.13	0.06	0	1.76	1.86
pancreatic endothelial cell	0.21	0.18	0	1.26	1.72
smooth muscle cell (heart)	0.26	0.2	0.4	1.18	0.83
stem cell of epidermis	0.22	0.06	0	1.47	0.8
astrocyte	0.1	1.19	0	1.96	1.19
B cell	0.2	0.04	0	0.85	0.75
B cell (fat)	0.15	0.05	0	0.19	0.21
B cell (limb)	0.24	0	0	0.28	0.16
B cell (liver)	0.2	0.04	0	0.21	0.11
B cell (lung)	0.19	0.04	0	0.13	0.22
B cell (spleen)	0.12	0.02	0	0.31	0.24
blood cell (trachea)	0.07	0.73	0	1.3	1.1
brush cell of epithelium proper of large intestine	0.09	0.11	0	0.95	0.52
DNAi1 myoblast pro-T cell	0.14	0.13	0	0.81	0.45
endothelial cell of hepatic sinusoid	0.72	0.06	0	1.45	0.69
enterocyte of epithelium of large intestine	0.1	0.01	0.01	0.88	0.05
enteroendocrine cell	0.05	0.45	0	1.4	1.16
epithelial cell of large intestine	0.06	0.19	0	1.28	1.07
epithelial cell of proximal tubule	0.12	0.11	0.01	0.95	0.31
hepatocyte	0.19	0.13	0	1.02	1.49
immature B cell	0.05	0.08	0	0.44	0.56
immature natural killer cell	0.22	0.18	0	1.56	0.85
immature NK T cell	0.07	0.18	0	0.75	0.87
immature T cell (bone marrow)	0.06	0.02	0	0.48	0.49
immature T cell (thymus)	0.1	0.03	0	0.84	1.05
keratinocyte (lung)	0.43	1.26	0	1.37	0.4
kidney collecting duct epithelial cell	0.25	0.43	0	0.56	0.22
Kupffer cell	0.18	0.1	0	0.67	0.61
large intestine goblet cell	0.05	0.22	0	1.44	0.37
large pro-B cell	0.08	0.25	0	0.95	0.93
leukocyte (blood)	0	0	0	0.11	0.28
leukocyte (lung)	0.14	0.07	0	1.56	1.13
leukocyte (pancreas)	0.17	0.3	0	0.87	0.92
macrophage (bone marrow)	0.03	0.19	0	0.85	0.93
macrophage (brain)	0.05	0.15	0	0.7	0.93
macrophage (kidney)	0.06	0.16	0	0.85	0.96
macrophage (limb)	0.62	0.24	0	1.34	1.12
macrophage (spleen)	0.11	0.03	0.03	0.94	0.76
mature natural killer cell	0.04	0.04	0	0.71	1.45
microglial cell	0.13	0.41	0	1.01	0.31
monocyte (lung)	0.13	0.07	0	0.54	0.88
myeloid cell (fat)	0.17	0.42	0	1.5	1.22
myeloid cell (lung)	0.56	0.75	0	0.87	1.14
NA (lung)	1.41	1.06	0	0.16	0.57
naive B cell	0.06	0.04	0	0.33	0.24
natural killer cell (fat)	0.1	0.05	0	0.45	0.52
natural killer cell (liver)	0.06	0.14	0.02	1.15	0.63
natural killer cell (lung)	0.39	0.11	0	0.4	0.38
oligodendrocyte	0.18	0.16	0	1.03	1.1
pancreatic acinar cell	0.23	0.07	0	0.23	0.2
precursor B cell	0.04	0.26	0	0.29	0.27
regulatory T cell	0.01	0.06	0	0.79	0.61
T cell (fat)	0.18	0.03	0	0.52	0.79
T cell (limb)	0.38	0.06	0	0.72	0.5
T cell (lung)	0.31	0.01	0	0.87	0.64
T cell (spleen)	0.11	0.02	0	0.71	0.48
thiocyte	0.24	0.01	0.06	0.72	0.86
thiocyte (skin)	0.05	0.06	0	0.75	0.96
ciliated columnar cell of tracheobronchial tree	0.3	0.07	0	0.53	1.78
pancreatic ductal cell	1	0.08	0	0.6	0.37
Bergmann glial cell	0.07	0.11	0	0.22	1.32
blastoid epithelial cell	0.16	0.14	0.01	0.85	0.21
classical monocyte (lung)	0.11	0.26	0	0.23	0.86
common lymphoid progenitor	0.1	0.56	0	0.54	1.64
fibroblast (heart)	1.12	0.47	0.12	0.18	0.89
granulocyte	0.1	0.02	0	0.03	0.33
granulocyte monocyte progenitor cell	0.05	0.08	0	0.2	0.1
hemopoietic precursor	0.08	0.14	0	0.26	1.2
leukocyte (heart)	0.24	0.42	0.01	0.39	1.42
luminal epithelial cell (breast)	0.78	0.06	0	0.53	0.14
megakaryocyte erythroid progenitor cell	0.03	0.17	0	0.79	1.78
monocyte (bone marrow)	0.03	0.56	0	0.25	0.72
NA (fat)	1.12	0.18	0	0.1	0.55
NA (heart)	0.22	0.72	0	0.25	0.92
neuron	0.23	0.33	0	1.71	1.68
pancreatic A cell	0.37	0.35	0	1.48	1.77
pancreatic D cell	0.06	0.16	0.02	0.97	0.95
pancreatic PP cell	0.04	0.19	0	0.74	0.87
pre-natural killer cell	0.05	0	0	1.15	0.5
Slamf1-negative multipotent progenitor cell	0.05	0.21	0	0.57	0.4
Slamf1-positive multipotent progenitor cell	0.03	0.36	0	0.45	0.82
type B pancreatic cell	0.09	0	0	1.41	1.67
cardiac muscle cell	0.26	0.95	0.06	0.57	0.81
basal cell (mammary)	0.26	0.01	0.01	0.71	0.71
epithelial cell of lung	1.35	0.06	0	1.62	1.52
leukocyte (thymus)	0.08	1.22	0	0.85	0.71
limb skeletal muscle satellite cell	0.43	0.33	0.02	1.15	0.64
mesenchymal cell (trachea)	0.23	1.45	0.05	0.25	0.84
mesenchymal stem cell (fat)	0.24	0.44	0.07	0.28	0.97
mesenchymal stem cell (limb)	0.7	0.55	0	0.23	0.86
myofibroblast cell	0.29	0.08	0	0.64	1.31
pancreatic stellate cell	0.18	1.37	0.31	0.76	0.31
skeletal muscle satellite stem cell	0.26	0.29	0	0.79	1.12
stromal cell (breast)	0.19	1.33	0.01	1.37	0.86
stromal cell (lung)	0.08	1.04	0.23	0.43	0.86
tracheal epithelial cell	1.46	1.11	0.08	0.88	1.32
basal cell of epidermis (skin)	0.37	0.01	0	1.43	0.41
basal cell of epidermis (lung)	0.75	0.46	0	1.15	1.42
brain endothelial cell	0.45	0.27	0	1.47	0.27
epidermal cell	0.26	0.06	0	1.1	1.16
keratinocyte stem cell	0.54	0.55	0	1.82	0.64
kidney endothelial cell	0.26	0.08	0	0.53	0.63
basophil	0.08	0.17	0	0.55	0.38
granulocyticopoietic cell	0.03	0.01	0	0.69	0.45
nicotinic endothelial cell	0.26	0.06	0.02	0	0
diaphragm endothelial cell	0.7	1.09	0	0	0
erythrocyte (aorta)	0.47	0.3	0.09	0	0
erythrocyte (heart)	0	0	0	0.13	0.31
fibroblast (aorta)	0.01	0.4	0.19	0	0
lymphocyte (diaphragm)	0.2	0.03	0	0.29	0.38
lymphocyte (limb)	0	0	0	0	0
macrophage (diaphragm)	0.19	0.44	0	0	0
mesenchymal stem cell	1.39	0.16	0.01	0	0
professional antigen presenting cell (aorta)	0.55	0.45	0.07	0	0
tracheal endothelial cell	0.45	0.34	0	1.23	0.74

Single-cell transcriptomics (cardioid-1, cardioid-2, cardioid-3, Pu010-1, Pu010-2)  
 (Data from: Single-cell transcriptomics (cardioid-1, cardioid-2, cardioid-3, Pu010-1, Pu010-2))



**Supplementary Table 1:** The heart smooth muscle cells may include "cardiac muscle" which according to historical knowledge are similar to cardiac type at the root of the pulmonary artery and vein. Clustering in 10 groups by five genes suffices to subgroup most endothelia into two heterogeneous groups, cardiac muscle cells, B and T cells; skeletal muscle cells were not included. QuickCluster was used at  $p < 0.05$  to generate 10 groups.